

# A linearized energy preserving finite element method for the dynamical incompressible magnetohydrodynamics equations

Huadong Gao<sup>\*</sup> and Weifeng Qiu<sup>†</sup>

January 8, 2018

## Abstract

We present and analyze a linearized finite element method (FEM) for the dynamical incompressible magnetohydrodynamics (MHD) equations. The finite element approximation is based on mixed conforming elements, where Taylor–Hood type elements are used for the Navier–Stokes equations and Nédélec edge elements are used for the magnetic equation. The divergence free conditions are weakly satisfied at the discrete level. Due to the use of Nédélec edge element, the proposed method is particularly suitable for problems defined on non-smooth and multi-connected domains. For the temporal discretization, we use a linearized scheme which only needs to solve a linear system at each time step. Moreover, the linearized mixed FEM is energy preserving. We establish an optimal error estimate under a very low assumption on the exact solutions and domain geometries. Numerical results which includes a benchmark lid-driven cavity problem are provided to show its effectiveness and verify the theoretical analysis.

**Keywords:** incompressible MHD equations, energy preserving, linearized methods, finite element method, error analysis.

**AMS subject classifications.** 65M12, 65M15, 65M60.

## 1 Introduction

In this paper, we consider the dynamical incompressible magnetohydrodynamics (MHD) equations, which is a coupled equation system of Navier–Stokes equations of fluid dynamics

---

<sup>\*</sup>School of Mathematics and Statistics, Huazhong University of Science and Technology, Wuhan 430074, Peoples Republic of China. [huadong@hust.edu.cn](mailto:huadong@hust.edu.cn). The work of the author was supported in part by a grant from the National Natural Science Foundation of China (NSFC) under grant No. 11501227.

<sup>†</sup>Department of Mathematics, City University of Hong Kong, 83 Tat Chee Avenue, Hong Kong, China. [weifeqiu@cityu.edu.hk](mailto:weifeqiu@cityu.edu.hk). The work of the author was supported by a grant from the Research Grants Council of the Hong Kong Special Administrative Region, China. (Project No. CityU 11304017)

and Maxwell's equations of electromagnetism via Lorentz's force and Ohm's Law, as follows

$$\begin{cases} \frac{\partial \mathbf{u}}{\partial t} - \frac{1}{R_e} \Delta \mathbf{u} + \mathbf{u} \cdot \nabla \mathbf{u} + \nabla p - S_c \mathbf{curl} \mathbf{B} \times \mathbf{B} = \mathbf{f}, & \mathbf{x} \in \Omega, \end{cases} \quad (1.1)$$

$$\begin{cases} \frac{\partial \mathbf{B}}{\partial t} + \frac{S_c}{R_m} \mathbf{curl}(\mathbf{curl} \mathbf{B}) - S_c \mathbf{curl}(\mathbf{u} \times \mathbf{B}) = \mathbf{0}, & \mathbf{x} \in \Omega, \end{cases} \quad (1.2)$$

$$\begin{cases} \nabla \cdot \mathbf{u} = 0, & \mathbf{x} \in \Omega, \end{cases} \quad (1.3)$$

$$\begin{cases} \nabla \cdot \mathbf{B} = 0, & \mathbf{x} \in \Omega, \end{cases} \quad (1.4)$$

with boundary conditions

$$\begin{cases} \mathbf{u} = \mathbf{0}, & \mathbf{x} \in \partial\Omega, \end{cases} \quad (1.5)$$

$$\begin{cases} \mathbf{B} \cdot \mathbf{n} = 0, & \mathbf{curl} \mathbf{B} \times \mathbf{n} = \mathbf{0}, & \mathbf{x} \in \partial\Omega, \end{cases} \quad (1.6)$$

and initial conditions

$$\mathbf{u}(\mathbf{x}, 0) = \mathbf{u}_0(\mathbf{x}), \quad \mathbf{B}(\mathbf{x}, 0) = \mathbf{B}_0(\mathbf{x}), \quad (1.7)$$

where  $\operatorname{div} \mathbf{u}_0(\mathbf{x}) = \operatorname{div} \mathbf{B}_0(\mathbf{x}) = 0$ . In the above dynamical incompressible MHD system,  $\mathbf{u}$  represents the velocity of the fluid flow,  $\mathbf{B}$  represents magnetic field,  $p$  represents the pressure and  $\mathbf{f}$  stands for the external body force term, respectively. In this paper we assume  $\Omega$  is a bounded Lipschitz polyhedral domain in  $\mathbb{R}^3$  (polygonal domain in  $\mathbb{R}^2$ ), which might not be convex or simply-connected. The dynamical incompressible MHD equation system is characterized by three parameters: the hydrodynamic Reynolds number  $R_e$ , the magnetic Reynolds number  $R_m$  and the coupling number  $S_c$ . Another commonly used boundary condition for equation (1.2) of  $\mathbf{B}$  is defined by

$$\mathbf{B} \times \mathbf{n} = \mathbf{0}, \quad \mathbf{x} \in \partial\Omega. \quad (1.8)$$

In addition, the boundary condition for  $\mathbf{B}$  might be of a mixed type, i.e., (1.6) is used on part of  $\partial\Omega$ , while (1.8) is used on the other part. However, we shall mainly consider the boundary condition (1.5)-(1.6) in this paper.

The dynamical incompressible MHD equations have attracted an amount of attention due to its important applications in modeling liquid metals [13, 27] and plasma physics [16]. We refer to the monograph [13] by Gerbeau, Le Bris and Lelièvre as a summary of recent progress for the MHD equations, which includes mathematical modeling, analysis and numerical methods. Mathematical analyses of the dynamical MHD model can be found in [10, 23, 32, 33] and reference therein. Global existence of weak solutions has been well established. Sermame and Temam proved the existence and uniqueness of local strong solution on regular domains [33]. There have been numerous works on numerical methods for the incompressible MHD equations, see [3, 14, 17, 21, 22, 25, 29, 31, 35]. Due to the nonlinear coupling of the unknowns, the divergence free constraints and the low regularity of the exact solutions, it is a challenging task to design efficient numerical schemes for the dynamical incompressible MHD equations. Several nonlinear schemes have been suggested, see [21, 22], where the motivation for using nonlinear scheme is to preserve the properties of the original equations as much as possible. For example, energy conservation can be preserved at the discrete level for nonlinear schemes studied in [21, 22]. However, a key observation on the two nonlinear terms

$$-S_c \mathbf{curl} \mathbf{B} \times \mathbf{B} \quad \text{in (1.1)}, \quad -S_c \mathbf{curl}(\mathbf{u} \times \mathbf{B}) \quad \text{in (1.2)},$$

tells that the weak formulation admit anti-symmetric structure. That is, the sum of the corresponding terms in the weak formulation

$$-S_c(\mathbf{curl} \mathbf{B} \times \mathbf{B}, \mathbf{v}), \quad -S_c(\mathbf{u} \times \mathbf{B}, \mathbf{curl} \mathbf{C}), \quad (1.9)$$

vanishes if we take  $\mathbf{v} = \mathbf{u}$  and  $\mathbf{C} = \mathbf{B}$ . By using this property, a careful linearization yields an energy preserving discretization, see the FEM system (2.4)-(2.6). We shall mention that [30, 35] also noticed this anti-symmetric structure in incompressible MHD equations. Another issue is the constraint  $\mathbf{div} \mathbf{B} = 0$ . For the ideal MHD flow problem, not guaranteeing  $\mathbf{div} \mathbf{B} = 0$  to round-off error may lead to nonphysical solutions, see the numerical report in [6] by Brackbill and Barnes. Motivated by this, some attempts in developing divergence free numerical methods can be found in [21, 22]. Hu, Ma and Xu suggested a mixed finite element method (FEM) in [22], where the current  $\mathbf{E} = \mathbf{curl} \mathbf{B} - \mathbf{u} \times \mathbf{B}$  was introduced as a new variable. The  $\mathbf{H}(\mathbf{curl})$  conforming Nédélec edge element is applied for the discretization of  $\mathbf{E}$ . By using  $\mathbf{H}(\mathbf{div})$  conforming Raviart–Thomas element to approximate  $\mathbf{B}$ , the authors in [22] proved that their scheme is divergence free on each element. It seems that the only disadvantage for this approach is the expensive computational costs, where vector elements are heavily used in the spatial discretization. For problems defined on simply-connected domain, another strategy to eliminate the divergence free constraint is to introduce a new variable  $\mathbf{A}$  such that  $\mathbf{B} = \mathbf{curl} \mathbf{A}$  and then solve the new dynamical MHD system of  $\mathbf{A}$ ,  $\mathbf{u}$  and  $p$ , see the scheme proposed in [21] by Hiptmair et al.. However, the ideal MHD model in [6] is essentially different with the incompressible MHD equations (1.1)-(1.7). To the best knowledge of the authors, there are no numerical reports which show that  $\mathbf{div} \mathbf{B}_h \neq 0$  leads to nonphysical solutions for (1.1)-(1.7). An alternative and less expensive way to deal with this constraint is to enforce the divergence free condition weakly. For example, in [31] the numerical solution  $\mathbf{B}_h$  satisfies

$$\int_{\Omega} \mathbf{B}_h \cdot \nabla v_h \, dx = 0, \quad \forall v_h \in V_h(\Omega)$$

where  $V_h(\Omega)$  denotes a certain FE space. Let us remark that this approach and its generalizations has been widely used, see [3, 11, 14, 17, 18, 20, 29, 30, 31, 35]. Finally, it should be noted that the regularity of  $\mathbf{B}$  on non-convex and non-smooth domains is lower than  $\mathbf{H}^1(\Omega)$ . Due to the  $\mathbf{curl} \mathbf{curl}$  structure of magnetic equation (1.2), it is well-known that on a general non-convex Lipschitz polyhedron [1, 12],  $\mathbf{H}(\mathbf{div}, \Omega) \cap \mathbf{H}(\mathbf{curl}, \Omega)$  is embedded in  $\mathbf{H}^s(\Omega)$  for  $\frac{1}{2} < s < 1$  only. However, conventional Lagrange FEMs for a scalar parabolic equation require the regularity of the exact solution in  $H^{1+s}(\Omega)$  with  $s > 0$  [8, 9]. Thus, analyses in [20, 35] all assume that the domain  $\Omega$  is convex or smooth to ensure the convergence of conventional Lagrange FEMs. To overcome this difficulty, the  $\mathbf{H}(\mathbf{curl})$  conforming Nédélec edge element can solve for the  $\mathbf{curl} \mathbf{curl}$  problem correctly on more general geometries, which has attracted much attention in the mathematical society and been successfully used in electromagnetics industry.

In this paper, we present a linearized mixed FEM for the dynamical incompressible MHD equations. Though the incompressible MHD equations (1.1)-(1.7) introduce strongly nonlinear coupling between  $\mathbf{u}$  and  $\mathbf{B}$ , a careful linearization for  $-S_c \mathbf{curl} \mathbf{B} \times \mathbf{B}$  in (1.1) and  $-S_c \mathbf{curl}(\mathbf{u} \times \mathbf{B})$  in (1.2) yields an energy preserving scheme, see the linearized FEM (2.4)-(2.6) in section 2. The cancellation of these two nonlinear terms plays a key role in later theoretical analysis. Moreover, the proposed scheme is linear. At each time step, we only need to solve a linear system which makes the proposed scheme very attractive in

practical computations. Limited work has been done for problems defined on non-convex domains when  $\mathbf{B}$  is not in  $\mathbf{H}^1(\Omega)$ . By using Nédélec edge element space, we obtain optimal error estimate for a linearized scheme under relatively low regularity assumption on the exact solution. In particular, the proposed scheme converges and the error analysis holds for problems defined on non-smooth, non-convex and multi-connected domains.

The rest of this paper is organized as follows. In section 2, we provide a linearized mixed FEM for the incompressible MHD equations. In section 3, we present analysis of the linearized scheme. Numerical examples for both two- and three-dimensional models are given in section 4 to show the efficiency of our method. Some concluding remarks are given in section 5.

## 2 A conservative linearized mixed FEM

### 2.1 Preliminaries

We now introduce notions for some standard Sobolev spaces. For any two functions  $u, v \in L^2(\Omega)$ , we denote the  $L^2(\Omega)$  inner product and norm by

$$(u, v) = \int_{\Omega} u(x) \cdot v(x) \, dx, \quad \|u\|_{L^2} = (u, u)^{\frac{1}{2}},$$

where  $\cdot$  denotes the inner product in case of vectorial functions. Let  $W^{k,p}(\Omega)$  be the Sobolev space defined on  $\Omega$ , and by conventional notations,  $H^k(\Omega) := W^{k,2}(\Omega)$ ,  $\mathring{H}^k(\Omega) := \mathring{W}^{k,2}(\Omega)$ . Let  $\mathbf{H}^k(\Omega) = [H^k(\Omega)]^d$  be a vector-valued Sobolev space, where  $d$  is the dimension of  $\Omega$ . For a positive real number  $s = k + \theta$  with  $0 < \theta < 1$ , we define  $H^s(\Omega) = (H^k, H^{k+1})_{[\theta]}$  by the complex interpolation, see [4]. For  $(\mathbf{u}, p)$ , we shall introduce

$$\mathring{\mathbf{H}}^1(\Omega) = \{\mathbf{u} \in \mathbf{H}^1(\Omega), \quad \mathbf{u}|_{\partial\Omega} = \mathbf{0}\}, \quad L_0^2 = \{u \in L^2, \quad (u, 1) = 0\}. \quad (2.1)$$

For the magnetic field  $\mathbf{B}$ , we denote

$$\mathbf{H}(\mathbf{curl}) = \{\mathbf{B} \mid \mathbf{B} \in \mathbf{L}^2(\Omega), \mathbf{curl} \mathbf{B} \in \mathbf{L}^2(\Omega)\} \text{ with } \|\mathbf{B}\|_{\mathbf{H}(\mathbf{curl})} = (\|\mathbf{B}\|_{L^2}^2 + \|\mathbf{curl} \mathbf{B}\|_{L^2}^2)^{\frac{1}{2}},$$

and its dual space  $\mathbf{H}(\mathbf{curl})'$  with norm

$$\|\mathbf{B}\|_{\mathbf{H}(\mathbf{curl})'} := \sup_{\mathbf{w} \in \mathbf{H}(\mathbf{curl})} \frac{(\mathbf{B}, \mathbf{w})}{\|\mathbf{w}\|_{\mathbf{H}(\mathbf{curl})}}.$$

Moreover, we denote

$$\mathbf{H}(\mathbf{div}) = \{\mathbf{A} \mid \mathbf{A} \in \mathbf{L}^2(\Omega), \mathbf{div} \mathbf{A} \in L^2(\Omega)\} \text{ with } \|\mathbf{A}\|_{\mathbf{H}(\mathbf{div})} = (\|\mathbf{A}\|_{L^2}^2 + \|\mathbf{div} \mathbf{A}\|_{L^2}^2)^{\frac{1}{2}}$$

Now we introduce some notations for the numerical methods. Let  $\mathcal{T}_h$  be a quasi-uniform tetrahedral partition of  $\Omega$  with  $\Omega = \cup_K \Omega_K$ . The mesh size is denoted by  $h = \max_{\Omega_K \in \mathcal{T}_h} \{\text{diam} \Omega_K\}$ . To approximate  $(\mathbf{u}, p)$ , we use the finite element pair

$$\mathbf{X}_h \subset \mathring{\mathbf{H}}^1(\Omega) \quad \text{and} \quad M_h \subset L_0^2(\Omega),$$

which satisfies the discrete inf-sup condition: there exists a constant  $\beta > 0$  such that

$$\inf_{0 \neq q_h \in M_h} \sup_{\mathbf{0} \neq \mathbf{v}_h \in \mathbf{X}_h} \frac{(q_h, \mathbf{div} \mathbf{v}_h)}{\|\mathbf{v}_h\|_{\mathbf{H}^1} \|q_h\|_{L^2}} \geq \beta_1, \quad (2.2)$$

where  $\beta_1$  depends on  $\Omega$  only. In this paper, we choose the popular generalized Taylor–Hood FE space  $\mathbf{X}_h^{k+1} \times M_h^k$  with  $k \geq 1$  for the approximation of  $(\mathbf{u}, p)$ , see [5, 15]. Here  $\mathbf{X}_h^{k+1}$  is the  $(k+1)$ -th order vectorial Lagrange FE space and  $M_h^k$  represents the  $k$ -th order scalar Lagrange FE subspace of  $L_0^2(\Omega)$ , respectively. We shall also introduce  $V_h^k$  to be the  $k$ -th order scalar Lagrange FE subspace of  $H^1(\Omega)$ . To approximate  $\mathbf{B}$ , we denote by  $\mathbf{Q}_h^k$  the  $k$ -th order first type Nédélec FE subspace of  $\mathbf{H}(\mathbf{curl})$ , where the case  $k = 1$  corresponds to the lowest order Nédélec edge element (6 dofs). We denote by  $\Pi_h$  a general projection operator on  $\mathbf{X}_h^k, M_h^k, \mathbf{Q}_h^k$  and  $V_h^k$ . The approximation properties of  $\Pi_h$  are summarized in the following lemma.

**Lemma 2.1** By noting the approximation properties of the finite element spaces  $\mathbf{X}_h^k, M_h^k$  (or  $V_h^k$ ) and  $\mathbf{Q}_h^k$ , we denote by  $\Pi_h$  the projection operator on  $\mathbf{X}_h^k, M_h^k$ , and  $\mathbf{Q}_h^k$ , satisfying

$$\begin{cases} \|\boldsymbol{\omega} - \Pi_h \boldsymbol{\omega}\|_{L^2} \leq Ch^s \|\boldsymbol{\omega}\|_{\mathbf{H}^s}, & 0 < s \leq k+1, \\ \|\omega - \Pi_h \omega\|_{L^2} \leq Ch^s \|\omega\|_{H^s}, & 0 < s \leq k+1, \\ \|\boldsymbol{\chi} - \Pi_h \boldsymbol{\chi}\|_{L^2} + \|\mathbf{curl}(\boldsymbol{\chi} - \Pi_h \boldsymbol{\chi})\|_{L^2} \leq Ch^s (\|\boldsymbol{\chi}\|_{H^s} + \|\mathbf{curl} \boldsymbol{\chi}\|_{H^s}), & \frac{1}{2} < s \leq k. \end{cases} \quad (2.3)$$

The interpolation results for Lagrange element space can be found in [7]. We refer to [26, Theorem 5.41] and [2] for the proof of the interpolation onto the Nédélec edge element space  $\mathbf{Q}_h^k$ . For the time discretization, let  $\{t_n\}_{n=0}^N$  be a uniform partition in the time direction with the step size  $\tau = \frac{T}{N}$ , and let  $u^n = u(\cdot, n\tau)$ . For a sequence of functions  $\{U^n\}_{n=0}^N$  defined on  $\Omega$ , we denote

$$D_\tau U^n = \frac{U^n - U^{n-1}}{\tau}, \quad \bar{U}^n = \frac{U^n + U^{n-1}}{2}, \quad \text{for } n = 1, 2, \dots, N.$$

## 2.2 A linearized mixed FEM

With the above notations, a linearized backward Euler mixed FEM for dynamical incompressible MHD equations (1.1)-(1.6) is to look for  $(\mathbf{u}_h^n, \mathbf{B}_h^n, p_h^n) \in \mathbf{X}_h^{k+1} \times \widehat{\mathbf{Q}}_h^k \times M_h^k$ , such that for any  $(\mathbf{v}_h^n, \mathbf{C}_h^n, q_h^n) \in \mathbf{X}_h^{k+1} \times \widehat{\mathbf{Q}}_h^k \times M_h^k$

$$\begin{cases} (D_\tau \mathbf{u}_h^n, \mathbf{v}_h) + \frac{1}{R_e} (\nabla \bar{\mathbf{u}}_h^n, \nabla \mathbf{v}_h) + \frac{1}{2} [(\mathbf{u}_h^{n-1} \cdot \nabla \bar{\mathbf{u}}_h^n, \mathbf{v}_h) - (\mathbf{u}_h^{n-1} \cdot \nabla \mathbf{v}_h, \bar{\mathbf{u}}_h^n)] \\ \quad - (p_h^n, \nabla \cdot \mathbf{v}_h) - S_c (\mathbf{curl} \bar{\mathbf{B}}_h^n \times \mathbf{B}_h^{n-1}, \mathbf{v}_h) = (\mathbf{f}^n, \mathbf{v}_h), & (2.4) \\ (D_\tau \mathbf{B}_h^n, \mathbf{C}_h) + \frac{S_c}{R_m} (\mathbf{curl} \bar{\mathbf{B}}_h^n, \mathbf{curl} \mathbf{C}_h) - S_c (\bar{\mathbf{u}}_h^n \times \mathbf{B}_h^{n-1}, \mathbf{curl} \mathbf{C}_h) = 0, & (2.5) \\ (\nabla \cdot \bar{\mathbf{u}}_h^n, q_h) = 0, & (2.6) \end{cases}$$

where  $k, \widehat{k} \geq 1$ . At the initial time step,  $\mathbf{u}_h^n = \Pi_h \mathbf{u}_0$  and  $\mathbf{B}_h^n = \Pi_h \mathbf{B}_0$ . We give several remarks concerning the proposed scheme.

**Remark 2.1** The above linearized mixed FEM (2.4)-(2.6) can be written in matrix form as

$$\begin{bmatrix} \frac{1}{\tau} \mathbf{M}_1 + \frac{1}{2R_e} \mathbf{K}_1 + \frac{1}{2} \mathbf{N}_1(\mathbf{u}_h^{n-1}) & \mathbf{B} & \frac{S_c}{2} \mathbf{N}_2(\mathbf{B}_h^{n-1}) \\ & \mathbf{B}^T & 0 \\ & & 0 \\ \frac{S_c}{2} \mathbf{N}_2^T(\mathbf{B}_h^{n-1}) & 0 & \frac{1}{\tau} \mathbf{M}_2 + \frac{S_c}{2R_m} \mathbf{K}_2 \end{bmatrix} \begin{bmatrix} \mathbf{u}_h^n \\ p_h^n \\ \mathbf{B}_h^n \end{bmatrix} := \mathbf{Ax} = \mathbf{b}, \quad (2.7)$$

with  $(p_h^n, 1) = 0$ . In terms of basis functions  $\{\phi\}_{i=1}^{N_h}$ , the block matrices in (2.7) are generated by

$$\begin{aligned}
\{\mathbf{M}_1\}_{i,j} &: (\phi_j, \phi_i), \quad \phi_i, \phi_j \in \mathbf{X}_h^k, \\
\{\mathbf{K}_1\}_{i,j} &: (\nabla \phi_j, \nabla \phi_i), \quad \phi_i, \phi_j \in \mathbf{X}_h^k, \\
\{\mathbf{N}_1\}_{i,j} &: \frac{1}{2} [(\mathbf{u}_h^{n-1} \cdot \nabla \phi_j, \phi_i) - (\mathbf{u}_h^{n-1} \cdot \nabla \phi_i, \phi_j)], \quad \phi_i, \phi_j \in \mathbf{X}_h^k, \\
\mathbf{B}_{i,j} &: -(\phi_j \nabla \cdot \phi_i), \quad \phi_j \in W_h^k, \quad \phi_i \in \mathbf{X}_h^k, \\
\{\mathbf{N}_2\}_{i,j} &: -(\mathbf{curl} \phi_j \times \mathbf{B}_h^{n-1}, \phi_i), \quad \phi_j \in \mathbf{Q}_h^k, \quad \phi_i \in \mathbf{X}_h^k, \\
\{\mathbf{M}_2\}_{i,j} &: (\phi_j, \phi_i), \quad \phi_i, \phi_j \in \mathbf{Q}_h^k, \\
\{\mathbf{K}_2\}_{i,j} &: (\mathbf{curl} \phi_j, \mathbf{curl} \phi_i), \quad \phi_i, \phi_j \in \widehat{\mathbf{Q}}_h^k.
\end{aligned}$$

To prove the existence and uniqueness of the linearized mixed FEM, it suffices to show that  $\mathbf{A}\mathbf{x} = 0$  admits zero solution only. Assuming  $\mathbf{A}\mathbf{x} = 0$ , then we have

$$0 = \mathbf{x}^T \mathbf{A}\mathbf{x} = \frac{1}{\tau} \|\mathbf{u}_h^n\|_{L^2}^2 + \frac{1}{2} R_e^{-1} \|\mathbf{u}_h^n\|_{L^2}^2 + \frac{1}{\tau} \|\mathbf{B}_h^n\|_{L^2}^2 + \frac{1}{2} S_c R_m^{-1} \|\mathbf{curl} \mathbf{B}_h^n\|_{L^2}^2, \quad (2.8)$$

from which  $\mathbf{u}_h^n = \mathbf{B}_h^n = \mathbf{0}$  follows directly. By using the inf-sup conditions (2.2), one can deduce that  $p_h^n = 0$ , which immediately leads to the fact that  $\mathbf{A}$  is invertible.

**Remark 2.2** In the above scheme, we only consider the homogeneous boundary condition (1.5)-(1.6). However, it should be noted that the proposed scheme is able to deal with the mixed type boundary condition for  $\mathbf{B}$  conveniently. For instance, we assume  $\partial\Omega = \Gamma_1 \cup \Gamma_2$  where  $\Gamma_1 \cap \Gamma_2 = \emptyset$ . The boundary condition for  $\mathbf{B}$  is set to be  $\mathbf{B} \times \mathbf{n} = \mathbf{0}$  on  $\Gamma_1$ , while  $\mathbf{B} \cdot \mathbf{n} = 0$  and  $\mathbf{curl} \mathbf{B} \times \mathbf{n} = \mathbf{0}$  on  $\Gamma_2$ . In this case, the FE space for  $\mathbf{B}$  shall be  $\{\mathbf{B}_h \in \widehat{\mathbf{Q}}_h^k \mid \mathbf{B}_h \times \mathbf{n} = \mathbf{0} \text{ on } \Gamma_1\}$ . The stability and error analyses also hold for problems with mixed type boundary conditions.

**Remark 2.3** The proposed scheme (2.4)-(2.6) satisfies a weakly divergence free property, namely, for any  $s_h \in V_h^k$ , taking  $\mathbf{C}_h^n = \nabla s_h$  in (2.5) gives

$$(D_\tau \mathbf{B}_h^n, \nabla s_h) = 0, \quad \text{for } n = 1, \dots, N,$$

which in turn leads to

$$(\mathbf{B}_h^n, \nabla s_h) = 0, \quad \forall s_h \in V_h^k \quad (2.9)$$

provided that  $(\mathbf{B}_h^0, \nabla s_h) = 0$ . Here, we have used the fact that  $\nabla V_h^k \subset \mathbf{Q}_h^k$ .

We present the Gagliardo–Nirenberg inequality and the discrete Gronwall’s inequality in the following lemmas which will be frequently used in our proofs.

**Lemma 2.2** (Gagliardo–Nirenberg inequality [28]): Let  $u$  be a function defined on  $\Omega$  in  $\mathbb{R}^d$  and  $\partial^s u$  be any partial derivative of  $u$  of order  $s$ , then

$$\|\partial^j u\|_{L^p} \leq C \|\partial^m u\|_{L^k}^a \|u\|_{L^q}^{1-a} + C \|u\|_{L^q},$$

for  $0 \leq j < m$  and  $\frac{j}{m} \leq a \leq 1$  with

$$\frac{1}{p} = \frac{j}{d} + a \left( \frac{1}{r} - \frac{m}{d} \right) + (1-a) \frac{1}{q},$$

except  $1 < r < \infty$  and  $m - j - \frac{d}{r}$  is a non-negative integer, in which case the above estimate holds only for  $\frac{j}{m} \leq a < 1$ .

**Lemma 2.3** Discrete Gronwall's inequality [19] : Let  $\tau, B$  and  $a_k, b_k, c_k, \gamma_k$ , for integers  $k \geq 0$ , be non-negative numbers such that

$$a_J + \tau \sum_{k=0}^J b_k \leq \tau \sum_{k=0}^J \gamma_k a_k + \tau \sum_{k=0}^J c_k + B, \quad \text{for } J \geq 0,$$

suppose that  $\tau\gamma_k < 1$ , for all  $k$ , and set  $\sigma_k = (1 - \tau\gamma_k)^{-1}$ . Then

$$a_J + \tau \sum_{k=0}^J b_k \leq \exp\left(\tau \sum_{k=0}^J \gamma_k \sigma_k\right) \left(\tau \sum_{k=0}^J c_k + B\right), \quad \text{for } J \geq 0.$$

### 3 Analysis of the linearized mixed FEM

#### 3.1 Stability Analysis

**Theorem 3.1** For any  $(\mathbf{u}, p, \mathbf{B})$  that satisfy the dynamical incompressible MHD equations (1.1)-(1.6), the following estimate holds

$$\frac{1}{2} \frac{d}{dt} \|\mathbf{u}\|_{L^2}^2 + \frac{1}{2} \frac{d}{dt} \|\mathbf{B}\|_{L^2}^2 + \frac{1}{R_e} \|\nabla \mathbf{u}\|_{L^2}^2 + \frac{S_c}{R_m} \|\mathbf{curl} \mathbf{B}\|_{L^2}^2 = (\mathbf{f}, \mathbf{u}). \quad (3.1)$$

**Proof.** A standard energy estimate yields the desired results. ■

For the linearized FEM equations (2.4)-(2.6), we can prove the following theorem, which can be viewed as the discrete version of Theorem 3.1.

**Theorem 3.2** The numerical solutions  $(\mathbf{u}_h^n, p_h^n, \mathbf{B}_h^n)$  to the linearized mixed FEM (2.4)-(2.6) satisfy the following energy preserving property

$$\begin{aligned} & \|\mathbf{u}_h^n\|_{L^2}^2 + \|\mathbf{B}_h^n\|_{L^2}^2 + 2\tau \frac{1}{R_e} \|\nabla \bar{\mathbf{u}}_h^n\|_{L^2}^2 + 2\tau \frac{S_c}{R_m} \|\mathbf{curl} \bar{\mathbf{B}}_h^n\|_{L^2}^2 \\ & = \|\mathbf{u}_h^{n-1}\|_{L^2}^2 + \|\mathbf{B}_h^{n-1}\|_{L^2}^2 + 2\tau (\mathbf{f}^n, \bar{\mathbf{u}}_h^n), \end{aligned} \quad (3.2)$$

which further results in the following energy stability

$$\begin{aligned} & \max_{0 \leq j \leq n} \left( \|\mathbf{u}_h^j\|_{L^2}^2 + \|\mathbf{B}_h^j\|_{L^2}^2 \right) + \sum_{j=1}^n \tau \left( \frac{1}{R_e} \|\nabla \bar{\mathbf{u}}_h^j\|_{L^2}^2 + \frac{S_c}{R_m} \|\mathbf{curl} \bar{\mathbf{B}}_h^j\|_{L^2}^2 \right) \\ & \leq \|\mathbf{u}_h^0\|_{L^2}^2 + \|\mathbf{B}_h^0\|_{L^2}^2 + C \sum_{j=1}^n \tau \|\mathbf{f}^{j+1}\|_{H^{-1}}^2. \end{aligned} \quad (3.3)$$

**Proof.** By taking  $\mathbf{v}_h = \bar{\mathbf{u}}_h^n$  into (2.4),  $\mathbf{C}_h = \bar{\mathbf{B}}_h^n$  into (2.5) and  $q_h = p_h^n$  into (2.6), respectively, and summing up the results, we obtain (3.2). By using the discrete Gronwall's inequality, we can prove (3.3). ■

**Remark 3.1** We shall note that Theorem 3.2 does not depend on the choice of the finite element space. If other boundary conditions are used, energy preserving property can be proved similarly.

### 3.2 Error analysis of the linearized FEM

To do the error estimate, we assume that the initial-boundary value problem (1.1)-(1.7) has a unique solution satisfying the regularity assumption below

$$\begin{cases} \mathbf{u} \in L^\infty(0, T; \mathbf{H}^{l+1}), \mathbf{u}_t \in L^\infty(0, T; \mathbf{H}^{l+1}), \mathbf{u}_{tt} \in L^2(0, T; \mathbf{L}^2) \\ p \in L^\infty(0, T; H^l), p_t \in L^\infty(0, T; H^l), \end{cases} \quad (3.1)$$

and

$$\begin{cases} \mathbf{B} \in L^\infty(0, T; \mathbf{H}^l), \mathbf{B}_t \in L^\infty(0, T; \mathbf{H}^l), \mathbf{B}_{tt} \in L^2(0, T; \mathbf{L}^2), \\ \mathbf{curl} \mathbf{B} \in L^\infty(0, T; \mathbf{H}^l), \mathbf{curl} \mathbf{B}_t \in L^\infty(0, T; \mathbf{H}^l), \end{cases} \quad (3.2)$$

where  $l > \frac{1}{2}$  depends on the regularity of the domain  $\Omega$ . In the rest part of this paper, for simplicity of notation we denote by  $C$  a generic positive constant and  $\epsilon$  a generic small positive constant, which are independent of  $j$ ,  $h$  and  $\tau$ . We present our main results on error estimates in the following theorem.

**Theorem 3.3** Suppose that the incompressible MHD system (1.1)-(1.7) has a unique solution  $(\mathbf{u}, p, \mathbf{B})$  satisfying the regularity (3.2). Then the linearized backward Euler mixed FEM (2.4)-(2.6) admits a unique solution  $(\mathbf{u}_h^n, p_h^n, \mathbf{B}_h^n) \in \mathbf{X}_h^{k+1} \times \mathbf{Q}_h^{\hat{k}} \times M_h^k$  for  $n = 1, \dots, N$ , and there exist two positive constants  $\tau_0$  and  $h_0$  such that when  $\tau < \tau_0$  and  $h \leq h_0$

$$\begin{aligned} & \max_{0 \leq n \leq N} \left( \|\mathbf{u}_h^n - \mathbf{u}^n\|_{L^2}^2 + \|\mathbf{B}_h^n - \mathbf{B}^n\|_{L^2}^2 \right) \\ & + \tau \sum_{m=1}^N \left( \|\nabla(\bar{\mathbf{u}}_h^m - \bar{\mathbf{u}}^m)\|_{L^2}^2 + \|\mathbf{curl}(\bar{\mathbf{B}}_h^m - \bar{\mathbf{B}}^m)\|_{L^2}^2 \right) \leq C_*(\tau^2 + h^{2s}), \end{aligned} \quad (3.3)$$

with  $s = \min\{k, \hat{k}, l\}$ , where  $\hat{k}$  and  $k$  are the order index of the finite element spaces,  $l$  is the index of regularity of the exact solutions. In (3.3),  $C_*$  is a positive constant independent of  $n$ ,  $h$  and  $\tau$ .

#### 3.2.1 The Stokes projection and some error bounds

To do error analysis, we shall introduce the Stokes projection  $\mathbf{R}_h : (\mathring{\mathbf{H}}^1, L_0^2) \rightarrow (\mathbf{X}_h^{k+1}, M_h^k)$ . For given  $t \in (0, T]$ , we look for  $\mathbf{R}_h(\mathbf{u}, p) := (\mathbf{R}_h(\mathbf{u}, p)_1, \mathbf{R}_h(\mathbf{u}, p)_2) \in (\mathbf{X}_h^{k+1}, M_h^k)$  such that

$$\begin{cases} \frac{1}{Re}(\nabla(\mathbf{R}_h(\mathbf{u}, p)_1 - \mathbf{u}), \nabla \mathbf{v}_h) - (\mathbf{R}_h(\mathbf{u}, p)_2 - p, \nabla \cdot \mathbf{v}_h) = 0, & \forall \mathbf{v}_h \in \mathbf{X}_h^{k+1}, \\ (\nabla \cdot (\mathbf{R}_h(\mathbf{u}, p)_1 - \mathbf{u}), q_h) = 0, & \forall q_h \in M_h^k. \end{cases} \quad (3.4)$$

For simplicity, we denote

$$R_h \mathbf{u} = \mathbf{R}_h(\mathbf{u}, p)_1, \quad R_h p = \mathbf{R}_h(\mathbf{u}, p)_2,$$

Theoretical analysis on convergence and stability of the above projections can be found in [15]. We summarize the main results in the following lemma.

**Lemma 3.1** For the projections defined above, the following error estimates hold

$$\|R_h \mathbf{u} - \mathbf{u}\|_{\mathbf{H}^1} + \|R_h p - p\|_{L^2} \leq C \left( \inf_{\mathbf{v}_h \in \mathbf{X}_h^{k+1}} \|\mathbf{v}_h - \mathbf{u}\|_{\mathbf{H}^1} + \inf_{q_h \in M_h^k} \|q_h - p\|_{L^2} \right), \quad (3.5)$$

We denote the projection errors of  $(\mathbf{u}, p)$  and interpolation error of  $\mathbf{B}$  by

$$\theta_{\mathbf{u}} = R_h \mathbf{u} - \mathbf{u}, \quad \theta_p = R_h p - p, \quad \theta_{\mathbf{B}} = \Pi_h \mathbf{B} - \mathbf{B}.$$

Then, by the regularity assumption (3.2) and Lemma 3.1, we have

$$\|\theta_{\mathbf{u}}\|_{H^1} + \|\theta_p\|_{L^2} \leq Ch^s (\|\mathbf{u}\|_{H^{1+s}} + \|p\|_{H^s}), \quad (3.6)$$

$$\|\theta_{\mathbf{B}}\|_{\mathbf{H}(\mathbf{curl})} \leq Ch^s \|\mathbf{B}\|_{\mathbf{H}^s(\mathbf{curl})} \quad (3.7)$$

and

$$\begin{aligned} \left\| \frac{\partial \theta_{\mathbf{u}}}{\partial t} \right\|_{H^s} &\leq Ch^s \left( \left\| \frac{\partial \mathbf{u}}{\partial t} \right\|_{H^{1+s}} + \left\| \frac{\partial p}{\partial t} \right\|_{H^s} \right), \\ \left\| \frac{\partial \theta_{\mathbf{B}}}{\partial t} \right\|_{L^2} &\leq Ch^s \left( \left\| \frac{\partial \mathbf{B}}{\partial t} \right\|_{H^s} + \left\| \mathbf{curl} \frac{\partial \mathbf{B}}{\partial t} \right\|_{H^s} \right). \end{aligned} \quad (3.8)$$

Moreover, by using inverse inequalities we can deduce the following uniform boundedness for  $R_h \mathbf{u}$  and  $\Pi_h \mathbf{B}$

$$\|R_h \mathbf{u}\|_{\infty} + \|R_h \mathbf{u}\|_{W^{1,3}} \leq C (\|\mathbf{u}\|_{H^{1+l}} + \|p\|_{H^l}) \leq C. \quad (3.9)$$

$$\|\Pi_h \mathbf{B}\|_{L^3} + \|\mathbf{curl} \Pi_h \mathbf{B}\|_{L^3} \leq C (\|\mathbf{B}\|_{H^l} + \|\mathbf{curl} \mathbf{B}\|_{H^l}) \leq C. \quad (3.10)$$

where  $l > \frac{1}{2}$  in the regularity assumption (3.1)-(3.2).

With the above projection error estimates we only need to estimate the following error equations

$$e_{\mathbf{u}}^n = \mathbf{u}_h^n - R_h \mathbf{u}^n, \quad e_p^n = p_h^n - R_h p^n, \quad e_{\mathbf{B}}^n = \mathbf{B}_h^n - R_h \mathbf{B}^n \quad (3.11)$$

for  $n = 0, 1, \dots, N$ .

### 3.2.2 The proof of the error estimate in Theorem 3.3

**Proof.** At the initial time step, we have

$$\|e_{\mathbf{u}}^0\|_{L^2}^2 + \|e_{\mathbf{B}}^0\|_{L^2}^2 \leq Ch^{2s}.$$

By the projection (3.4) and the regularity assumption (3.2), one can verify that the exact solution satisfies the formulation below

$$\begin{cases} (D_{\tau} \mathbf{u}^n, \mathbf{v}_h) + \frac{1}{R_e} (\nabla R_h \bar{\mathbf{u}}^n, \nabla \mathbf{v}_h) + \frac{1}{2} [(\mathbf{u}^{n-1} \cdot \nabla \bar{\mathbf{u}}^n, \mathbf{v}_h) - (\mathbf{u}^{n-1} \cdot \nabla \mathbf{v}_h, \bar{\mathbf{u}}^n)] \\ \quad - (R_h p^n, \nabla \cdot \mathbf{v}_h) - S_c(\mathbf{curl} \bar{\mathbf{B}}^n \times \mathbf{B}^{n-1}, \mathbf{v}_h) = (\mathbf{f}^n, \mathbf{v}_h) + R_1(\mathbf{v}_h), \end{cases} \quad (3.12)$$

$$(\nabla \cdot R_h \bar{\mathbf{u}}^n, q_h) = 0, \quad (3.13)$$

$$(D_{\tau} \mathbf{B}^n, \mathbf{C}_h) + \frac{S_c}{R_m} (\mathbf{curl} \Pi_h \bar{\mathbf{B}}^n, \mathbf{curl} \mathbf{C}_h) - S_c(\bar{\mathbf{u}}^n \times \mathbf{B}^{n-1}, \mathbf{curl} \mathbf{C}_h) = R_2(\mathbf{C}_h), \quad (3.14)$$

for any  $(\mathbf{v}_h, q_h, \mathbf{C}_h) \in \mathbf{X}_h^k \times M_h^k \times \mathbf{Q}_h^{\hat{k}}$ . Here the two truncation error terms are defined by

$$R_1(\mathbf{v}_h) = (D_{\tau} \mathbf{u}^n - \frac{\partial \mathbf{u}}{\partial t}(\mathbf{x}, t^n), \mathbf{v}_h) + \frac{1}{R_e} (\nabla (R_h \bar{\mathbf{u}}^n - R_h \mathbf{u}^n), \nabla \mathbf{v}_h)$$

$$\begin{aligned}
& + \left( \frac{1}{2} [(\mathbf{u}^{n-1} \cdot \nabla \bar{\mathbf{u}}^n, \mathbf{v}_h) - (\mathbf{u}^{n-1} \cdot \nabla \mathbf{v}_h, \bar{\mathbf{u}}^n)] - (\mathbf{u}^n \cdot \nabla \mathbf{u}^n, \mathbf{v}_h) \right) \\
& + S_c(\mathbf{curl} \mathbf{B}^n \times \mathbf{B}^n - \bar{\mathbf{B}}^n \times \mathbf{B}^{n-1}, \mathbf{v}_h), \tag{3.15}
\end{aligned}$$

$$\begin{aligned}
R_2(\mathbf{C}_h) & = (D_\tau \mathbf{B}^n - \frac{\partial \mathbf{B}}{\partial t}(\mathbf{x}, t^n), \mathbf{C}_h) + S_c R_m^{-1}(\mathbf{curl}(\Pi_h \bar{\mathbf{B}}^n - \mathbf{B}^n), \mathbf{curl} \mathbf{C}_h) \\
& + S_c(\mathbf{u}^n \times \mathbf{B}^n - \bar{\mathbf{u}}^n \times \mathbf{B}^{n-1}, \mathbf{curl} \mathbf{C}_h). \tag{3.16}
\end{aligned}$$

Then, subtracting (3.12)-(3.14) from the FEM system (2.4)-(2.6) gives the error equations

$$\begin{aligned}
& (D_\tau e_{\mathbf{u}}^n, \mathbf{v}_h) + R_e^{-1}(\nabla \bar{e}_{\mathbf{u}}^n, \nabla \mathbf{v}_h) - (e_p^n, \nabla \cdot \mathbf{v}_h) \\
& = \frac{1}{2} \left( [(\mathbf{u}^{n-1} \cdot \nabla \bar{\mathbf{u}}^n, \mathbf{v}_h) - (\mathbf{u}^{n-1} \cdot \nabla \mathbf{v}_h, \bar{\mathbf{u}}^n)] - [(\mathbf{u}_h^{n-1} \cdot \nabla \bar{\mathbf{u}}_h^n, \mathbf{v}_h) - (\mathbf{u}_h^{n-1} \cdot \nabla \mathbf{v}_h, \bar{\mathbf{u}}_h^n)] \right) \\
& + (S_c(\mathbf{curl} \bar{\mathbf{B}}_h^n \times \mathbf{B}_h^{n-1}, \mathbf{v}_h) - S_c(\mathbf{curl} \bar{\mathbf{B}}^n \times \mathbf{B}^{n-1}, \bar{\mathbf{v}}_h)) - (D_\tau \theta_{\mathbf{u}}^n, \mathbf{v}_h) - R_1(\mathbf{v}_h), \tag{3.17}
\end{aligned}$$

$$(\nabla \cdot \bar{e}_{\mathbf{u}}^n, q_h) = 0, \tag{3.18}$$

$$\begin{aligned}
& (D_\tau e_{\mathbf{B}}^n, \mathbf{C}_h) + S_c R_m^{-1}(\mathbf{curl} \bar{e}_{\mathbf{B}}^n, \mathbf{curl} \mathbf{C}_h) \\
& = S_c(\bar{\mathbf{u}}_h^n \times \mathbf{B}_h^{n-1} - \bar{\mathbf{u}}^n \times \mathbf{B}^{n-1}, \mathbf{curl} \mathbf{C}_h) - (D_\tau \theta_{\mathbf{B}}^n, \mathbf{C}_h) - R_2(\mathbf{C}_h), \tag{3.19}
\end{aligned}$$

for any  $(\mathbf{v}_h, q_h, \mathbf{C}_h) \in \mathbf{X}_h^k \times M_h^k \times \mathbf{Q}_h^{\widehat{k}}$ . We take  $\mathbf{v}_h = \bar{e}_{\mathbf{u}}^n$  in (3.17),  $q_h = e_p^n$  in (3.18) and  $\mathbf{C}_h = \bar{e}_{\mathbf{B}}^n$  in (3.19), respectively, and summing up the results to derive that

$$\begin{aligned}
& (D_\tau e_{\mathbf{u}}^n, \bar{e}_{\mathbf{u}}^n) + (D_\tau e_{\mathbf{B}}^n, \bar{e}_{\mathbf{B}}^n) + R_e^{-1} \|\nabla \bar{e}_{\mathbf{u}}^n\|_{L^2}^2 + S_c R_m^{-1} \|\mathbf{curl} \bar{e}_{\mathbf{B}}^n\|_{L^2}^2 \\
& = -\frac{1}{2} \left\{ [(\mathbf{u}_h^{n-1} \cdot \nabla \bar{\mathbf{u}}_h^n, \bar{e}_{\mathbf{u}}^n) - (\mathbf{u}_h^{n-1} \cdot \nabla \bar{e}_{\mathbf{u}}^n, \bar{\mathbf{u}}_h^n)] - [(\mathbf{u}^{n-1} \cdot \nabla \bar{\mathbf{u}}^n, \bar{e}_{\mathbf{u}}^n) - (\mathbf{u}^{n-1} \cdot \nabla \bar{e}_{\mathbf{u}}^n, \bar{\mathbf{u}}^n)] \right\} \\
& + S_c(\mathbf{curl} \bar{\mathbf{B}}_h^n \times \mathbf{B}_h^{n-1} - \mathbf{curl} \bar{\mathbf{B}}^n \times \mathbf{B}^{n-1}, \bar{e}_{\mathbf{u}}^n) \\
& + S_c(\bar{\mathbf{u}}_h^n \times \mathbf{B}_h^{n-1} - \bar{\mathbf{u}}^n \times \mathbf{B}^{n-1}, \mathbf{curl} \bar{e}_{\mathbf{B}}^n) \\
& - (D_\tau \theta_{\mathbf{u}}^n, \bar{e}_{\mathbf{u}}^n) - (D_\tau \theta_{\mathbf{B}}^n, \bar{e}_{\mathbf{B}}^n) - R_1(\bar{e}_{\mathbf{u}}^n) - R_2(\bar{e}_{\mathbf{B}}^n) \\
& := I_1(\bar{e}_{\mathbf{u}}^n) + I_2(\bar{e}_{\mathbf{u}}^n) + I_3(\bar{e}_{\mathbf{B}}^n) - (D_\tau \theta_{\mathbf{u}}^n, \bar{e}_{\mathbf{u}}^n) - (D_\tau \theta_{\mathbf{B}}^n, \bar{e}_{\mathbf{B}}^n) - R_1(\bar{e}_{\mathbf{u}}^n) - R_2(\bar{e}_{\mathbf{B}}^n). \tag{3.20}
\end{aligned}$$

By noting the regularity assumption (3.1)-(3.2) and Lemma 3.1, the linear terms on the right hand side of (3.20) satisfy

$$\begin{aligned}
& \tau \sum_{m=1}^n \{-(D_\tau \theta_{\mathbf{u}}^m, \bar{e}_{\mathbf{u}}^m) - (D_\tau \theta_{\mathbf{B}}^m, \bar{e}_{\mathbf{B}}^m) - R_1(\bar{e}_{\mathbf{u}}^m) - R_2(\bar{e}_{\mathbf{B}}^m)\} \\
& \leq \tau \sum_{m=1}^n \{ \epsilon \|\bar{e}_{\mathbf{u}}^m\|_{H^1}^2 + \epsilon \|\mathbf{curl} \bar{e}_{\mathbf{B}}^m\|_{H^1}^2 + C \|e_{\mathbf{u}}^m\|_{L^2}^2 + C \|e_{\mathbf{B}}^m\|_{L^2}^2 + C \|e_{\mathbf{u}}^{n-1}\|_{L^2}^2 + C \|e_{\mathbf{B}}^{n-1}\|_{L^2}^2 \} \\
& + C \tau^2 + \epsilon^{-1} C h^{2s}. \tag{3.21}
\end{aligned}$$

Next, we estimate the three nonlinear terms one by one. The first term  $I_1(e_{\mathbf{u}}^n)$  can be rewritten by

$$\begin{aligned}
I_1(\bar{e}_{\mathbf{u}}^n) & = -\frac{1}{2} \left\{ (\mathbf{u}_h^{n-1} \cdot \nabla \bar{\mathbf{u}}_h^n - \mathbf{u}^{n-1} \cdot \nabla \bar{\mathbf{u}}^n, \bar{e}_{\mathbf{u}}^n) - [(\mathbf{u}_h^{n-1} \cdot \nabla \bar{e}_{\mathbf{u}}^n, \bar{\mathbf{u}}_h^n) - (\mathbf{u}^{n-1} \cdot \nabla \bar{e}_{\mathbf{u}}^n, \bar{\mathbf{u}}^n)] \right\} \\
& = -\frac{1}{2} \left( (e_{\mathbf{u}}^{n-1} + \theta_{\mathbf{u}}^{n-1}) \cdot \nabla \bar{\mathbf{u}}_h^n, \bar{e}_{\mathbf{u}}^n \right) - \frac{1}{2} (\mathbf{u}^{n-1} \cdot \nabla (\bar{e}_{\mathbf{u}}^n + \bar{\theta}_{\mathbf{u}}^n), \bar{e}_{\mathbf{u}}^n) \\
& + \frac{1}{2} (\mathbf{u}^{n-1} \cdot \nabla \bar{e}_{\mathbf{u}}^n, \bar{e}_{\mathbf{u}}^n + \bar{\theta}_{\mathbf{u}}^n) + \frac{1}{2} ((e_{\mathbf{u}}^{n-1} + \theta_{\mathbf{u}}^{n-1}) \cdot \nabla \bar{e}_{\mathbf{u}}^n, \bar{\mathbf{u}}_h^n)
\end{aligned}$$

$$:= \sum_{i=1}^4 J_i^n. \quad (3.22)$$

We now estimate  $\{J_i^n\}_{i=1}^4$ . The term  $J_1^n + J_4^n$  can be bounded by

$$\begin{aligned} J_1^n + J_4^n &= -\frac{1}{2} ((e_{\mathbf{u}}^{n-1} + \theta_{\mathbf{u}}^{n-1}) \cdot \nabla \bar{e}_{\mathbf{u}}^n, \bar{e}_{\mathbf{u}}^n) - \frac{1}{2} ((e_{\mathbf{u}}^{n-1} + \theta_{\mathbf{u}}^{n-1}) \cdot \nabla R_h \bar{\mathbf{u}}^n, \bar{e}_{\mathbf{u}}^n) \\ &\quad + \frac{1}{2} ((e_{\mathbf{u}}^{n-1} + \theta_{\mathbf{u}}^{n-1}) \cdot \nabla \bar{e}_{\mathbf{u}}^n, \bar{e}_{\mathbf{u}}^n) + \frac{1}{2} ((e_{\mathbf{u}}^{n-1} + \theta_{\mathbf{u}}^{n-1}) \cdot \nabla \bar{e}_{\mathbf{u}}^n, R_h \bar{\mathbf{u}}^n) \\ &= -\frac{1}{2} ((e_{\mathbf{u}}^{n-1} + \theta_{\mathbf{u}}^{n-1}) \cdot \nabla R_h \bar{\mathbf{u}}^n, \bar{e}_{\mathbf{u}}^n) + \frac{1}{2} ((e_{\mathbf{u}}^{n-1} + \theta_{\mathbf{u}}^{n-1}) \cdot \nabla \bar{e}_{\mathbf{u}}^n, R_h \bar{\mathbf{u}}^n) \\ &\leq C \|e_{\mathbf{u}}^{n-1} + \theta_{\mathbf{u}}^{n-1}\|_{L^2} \|R_h \bar{\mathbf{u}}^n\|_{W^{1,3}} \|\bar{e}_{\mathbf{u}}^n\|_{L^6} + C \|e_{\mathbf{u}}^{n-1} + \theta_{\mathbf{u}}^{n-1}\|_{L^2} \|\bar{e}_{\mathbf{u}}^n\|_{H^1} \|R_h \bar{\mathbf{u}}^n\|_{L^\infty} \\ &\leq C \|e_{\mathbf{u}}^{n-1} + \theta_{\mathbf{u}}^{n-1}\|_{L^2} \|\bar{e}_{\mathbf{u}}^n\|_{H^1} \\ &\leq \epsilon \|\bar{e}_{\mathbf{u}}^n\|_{H^1}^2 + \epsilon^{-1} C \|e_{\mathbf{u}}^{n-1}\|_{L^2}^2 + \epsilon^{-1} C h^{2s}, \end{aligned} \quad (3.23)$$

where we have used the uniform boundedness results for  $R_h \bar{\mathbf{u}}^n$  in (3.9). And  $J_2^n + J_3^n$  can be estimated directly

$$\begin{aligned} J_2^n + J_3^n &\leq C \|\mathbf{u}^{n-1}\|_{L^\infty} \|\bar{\theta}_{\mathbf{u}}^n\|_{H^1} \|\bar{e}_{\mathbf{u}}^n\|_{L^2} + C \|\mathbf{u}^{n-1}\|_{L^\infty} \|\bar{e}_{\mathbf{u}}^n\|_{H^1} \|\bar{\theta}_{\mathbf{u}}^n\|_{L^2} \\ &\leq C h^s \|\bar{e}_{\mathbf{u}}^n\|_{L^2} + C \|\bar{e}_{\mathbf{u}}^n\|_{H^1} h^s \\ &\leq \epsilon \|\bar{e}_{\mathbf{u}}^n\|_{H^1}^2 + \epsilon^{-1} C (\|e_{\mathbf{u}}^n\|_{L^2}^2 + \|e_{\mathbf{u}}^{n-1}\|_{L^2}^2 + h^{2s}). \end{aligned} \quad (3.24)$$

With the above estimates (3.23) and (3.24), we get the following estimate

$$I_1(\bar{e}_{\mathbf{u}}^n) \leq \epsilon \|\bar{e}_{\mathbf{u}}^n\|_{H^1}^2 + \epsilon^{-1} C (\|e_{\mathbf{u}}^n\|_{L^2}^2 + \|e_{\mathbf{u}}^{n-1}\|_{L^2}^2 + h^{2s}). \quad (3.25)$$

Then, we turn to estimate  $I_2(\bar{e}_{\mathbf{u}}^n)$  and  $I_3(\bar{e}_{\mathbf{B}}^n)$ , which can be rewritten by

$$\begin{aligned} I_2(\bar{e}_{\mathbf{u}}^n) &= S_c(\mathbf{curl} \bar{e}_{\mathbf{B}}^n \times \mathbf{B}_h^{n-1}, \bar{e}_{\mathbf{u}}^n) + S_c(\mathbf{curl} \Pi_h \bar{\mathbf{B}}^n \times \mathbf{B}_h^{n-1} - \mathbf{curl} \bar{\mathbf{B}}^n \times \mathbf{B}^{n-1}, \bar{e}_{\mathbf{u}}^n) \\ &= S_c(\mathbf{curl} \bar{e}_{\mathbf{B}}^n \times \mathbf{B}_h^{n-1}, \bar{e}_{\mathbf{u}}^n) + S_c(\mathbf{curl} \Pi_h \bar{\mathbf{B}}^n \times (e_{\mathbf{B}}^{n-1} + \theta_{\mathbf{B}}^{n-1}), \bar{e}_{\mathbf{u}}^n) \\ &\quad + S_c(\mathbf{curl} \bar{\theta}_{\mathbf{B}}^n \times \mathbf{B}^{n-1}, \bar{e}_{\mathbf{u}}^n), \\ I_3(\bar{e}_{\mathbf{B}}^n) &= S_c(\bar{e}_{\mathbf{u}}^n \times \mathbf{B}_h^{n-1}, \mathbf{curl} \bar{e}_{\mathbf{B}}^n) + S_c(R_h \bar{\mathbf{u}}^n \times \mathbf{B}_h^{n-1} - \bar{\mathbf{u}}^n \times \mathbf{B}^{n-1}, \mathbf{curl} \bar{e}_{\mathbf{B}}^n) \\ &= S_c(\bar{e}_{\mathbf{u}}^n \times \mathbf{B}_h^{n-1}, \mathbf{curl} \bar{e}_{\mathbf{B}}^n) + S_c(R_h \bar{\mathbf{u}}^n \times (e_{\mathbf{B}}^{n-1} + \theta_{\mathbf{B}}^{n-1}), \mathbf{curl} \bar{e}_{\mathbf{B}}^n) \\ &\quad + S_c(\bar{\theta}_{\mathbf{u}}^n \times \mathbf{B}^{n-1}, \mathbf{curl} \bar{e}_{\mathbf{B}}^n). \end{aligned}$$

By noting the fact that

$$S_c(\mathbf{curl} \bar{e}_{\mathbf{B}}^n \times \mathbf{B}_h^{n-1}, \bar{e}_{\mathbf{u}}^n) + S_c(\bar{e}_{\mathbf{u}}^n \times \mathbf{B}_h^{n-1}, \mathbf{curl} \bar{e}_{\mathbf{B}}^n) = 0,$$

we have

$$\begin{aligned} &I_2(\bar{e}_{\mathbf{u}}^n) + I_3(\bar{e}_{\mathbf{B}}^n) \\ &= S_c(\mathbf{curl} \Pi_h \bar{\mathbf{B}}^n \times (e_{\mathbf{B}}^{n-1} + \theta_{\mathbf{B}}^{n-1}), \bar{e}_{\mathbf{u}}^n) + S_c(\mathbf{curl} \bar{\theta}_{\mathbf{B}}^n \times \mathbf{B}^{n-1}, \bar{e}_{\mathbf{u}}^n) \\ &\quad + S_c(R_h \bar{\mathbf{u}}^n \times (e_{\mathbf{B}}^{n-1} + \theta_{\mathbf{B}}^{n-1}), \mathbf{curl} \bar{e}_{\mathbf{B}}^n) + S_c(\bar{\theta}_{\mathbf{u}}^n \times \mathbf{B}^{n-1}, \mathbf{curl} \bar{e}_{\mathbf{B}}^n) \\ &\leq C \|\mathbf{curl} \Pi_h \bar{\mathbf{B}}^n\|_{L^3} \|e_{\mathbf{B}}^{n-1} + \theta_{\mathbf{B}}^{n-1}\|_{L^2} \|\bar{e}_{\mathbf{u}}^n\|_{L^6} + C \|\mathbf{curl} \bar{\theta}_{\mathbf{B}}^n\|_{L^2} \|\mathbf{B}^{n-1}\|_{L^3} \|\bar{e}_{\mathbf{u}}^n\|_{L^6} \\ &\quad + C \|R_h \bar{\mathbf{u}}^n\|_{L^\infty} \|e_{\mathbf{B}}^{n-1} + \theta_{\mathbf{B}}^{n-1}\|_{L^2} \|\mathbf{curl} \bar{e}_{\mathbf{B}}^n\|_{L^2} + C \|\bar{\theta}_{\mathbf{u}}^n\|_{L^6} \|\mathbf{B}^{n-1}\|_{L^3} \|\mathbf{curl} \bar{e}_{\mathbf{B}}^n\|_{L^2} \end{aligned}$$

$$\begin{aligned}
&\leq C(\|e_{\mathbf{B}}^{n-1}\|_{L^2} + h^s)\|\bar{e}_{\mathbf{u}}^n\|_{H^1} + C(\|e_{\mathbf{B}}^{n-1}\|_{L^2} + h^s)\|\mathbf{curl}\bar{e}_{\mathbf{B}}^n\|_{L^2} + Ch^s\|\mathbf{curl}\bar{e}_{\mathbf{B}}^n\|_{L^2} \\
&\leq \epsilon\|\bar{e}_{\mathbf{u}}^n\|_{H^1}^2 + \epsilon\|\mathbf{curl}\bar{e}_{\mathbf{B}}^n\|_{L^2}^2 + \epsilon^{-1}C\|e_{\mathbf{B}}^{n-1}\|_{L^2}^2 + \epsilon^{-1}Ch^{2s}, \tag{3.26}
\end{aligned}$$

where we have used the uniform boundedness of  $\Pi_h\mathbf{B}$  in (3.10). Finally, taking estimates (3.25) and (3.26) into (3.20), we arrive at

$$\begin{aligned}
&\frac{\|e_{\mathbf{u}}^n\|_{L^2}^2 - \|e_{\mathbf{u}}^{n-1}\|_{L^2}^2}{2\tau} + \frac{\|e_{\mathbf{B}}^n\|_{L^2}^2 - \|e_{\mathbf{B}}^{n-1}\|_{L^2}^2}{2\tau} + \frac{1}{R_e}\|\nabla\bar{e}_{\mathbf{u}}^n\|_{L^2}^2 + \frac{S_c}{R_m}\|\mathbf{curl}\bar{e}_{\mathbf{B}}^n\|_{L^2}^2 \\
&\leq \epsilon\|\bar{e}_{\mathbf{u}}^n\|_{H^1}^2 + \epsilon\|\mathbf{curl}\bar{e}_{\mathbf{B}}^n\|_{L^2}^2 + \epsilon^{-1}C\|e_{\mathbf{u}}^n\|_{L^2}^2 + \epsilon^{-1}C\|e_{\mathbf{u}}^{n-1}\|_{L^2}^2 + C\|e_{\mathbf{B}}^{n-1}\|_{L^2}^2 + \epsilon^{-1}C\tau^2 \\
&\quad + \epsilon^{-1}Ch^{2s} - (D_\tau\theta_{\mathbf{u}}^n, \bar{e}_{\mathbf{u}}^n) - (D_\tau\theta_{\mathbf{B}}^n, \bar{e}_{\mathbf{B}}^n) - R_1(\bar{e}_{\mathbf{u}}^n) - R_2(\bar{e}_{\mathbf{B}}^n). \tag{3.27}
\end{aligned}$$

Then, we chose a small  $\epsilon$  and sum up the last inequality for the index  $n = 0, 1, \dots, k$  to derive that

$$\begin{aligned}
&\|e_{\mathbf{u}}^n\|_{L^2}^2 + \|e_{\mathbf{B}}^n\|_{L^2}^2 + \tau \sum_{m=1}^n (\|\bar{e}_{\mathbf{u}}^m\|_{H^1}^2 + \|\mathbf{curl}\bar{e}_{\mathbf{B}}^m\|_{L^2}^2) \\
&\leq \tau \sum_{m=0}^n (\|e_{\mathbf{u}}^m\|_{L^2}^2 + C\|e_{\mathbf{B}}^m\|_{L^2}^2) + C\tau^2 + Ch^{2s} \tag{3.28}
\end{aligned}$$

where we have used the estimates (3.21) for the linear terms. By the discrete Gronwall's inequality in Lemma 2.3, when  $C\tau \leq \frac{1}{2}$ , we have

$$\begin{aligned}
&\|e_{\mathbf{u}}^n\|_{L^2}^2 + \|e_{\mathbf{B}}^n\|_{L^2}^2 + \tau \sum_{m=1}^n (\|\bar{e}_{\mathbf{u}}^m\|_{H^1}^2 + \|\mathbf{curl}\bar{e}_{\mathbf{B}}^m\|_{L^2}^2) \\
&\leq C \exp\left(\frac{TC}{1-C\tau}\right)(\tau^2 + h^{2s+2}) \\
&\leq C \exp(2TC)(\tau^2 + h^{2s+2}). \tag{3.29}
\end{aligned}$$

Theorem 3.3 is proved by combining (3.29) and the projection error estimates in Lemma 3.1.  $\blacksquare$

## 4 Numerical results

In this section, we provide some numerical experiments to confirm our theoretical analyses and demonstrate the accuracy, stability and robustness of the proposed linearized conservative FEM. The computations are performed with FEniCS [24].

### 4.1 Two-dimensional numerical results

We introduce several two-dimensional operators first. For scalar function  $p$  and vector function  $\mathbf{B} = [B_1, B_2]^T$ , the two-dimensional operators  $\text{div}$ ,  $\nabla$ ,  $\text{curl}$  and  $\mathbf{curl}$  are defined by

$$\nabla \cdot \mathbf{B} = \frac{\partial B_1}{\partial x} + \frac{\partial B_2}{\partial y}, \quad \nabla p = \left[ \frac{\partial p}{\partial x}, \frac{\partial p}{\partial y} \right]^T, \quad \text{curl } \mathbf{B} = \frac{\partial B_2}{\partial x} - \frac{\partial B_1}{\partial y}, \quad \mathbf{curl} p = \left[ \frac{\partial p}{\partial y}, -\frac{\partial p}{\partial x} \right]^T.$$

In two dimensional space, the dynamical incompressible MHD equations can be reduced to

$$\begin{cases} \frac{\partial \mathbf{u}}{\partial t} - \frac{1}{R_e} \Delta \mathbf{u} + \mathbf{u} \cdot \nabla \mathbf{u} + \nabla p - S_c \operatorname{curl} \mathbf{B} \begin{bmatrix} -B_2 \\ B_1 \end{bmatrix} = \mathbf{f}, & \mathbf{x} \in \Omega, \end{cases} \quad (4.1)$$

$$\begin{cases} \frac{\partial \mathbf{B}}{\partial t} + \frac{S_c}{R_m} \operatorname{curl} (\operatorname{curl} \mathbf{B}) - S_c \operatorname{curl} (u_1 B_2 - u_2 B_1) = \mathbf{0}, & \mathbf{x} \in \Omega, \end{cases} \quad (4.2)$$

$$\begin{cases} \nabla \cdot \mathbf{u} = 0, & \mathbf{x} \in \Omega, \end{cases} \quad (4.3)$$

$$\begin{cases} \nabla \cdot \mathbf{B} = 0, & \mathbf{x} \in \Omega, \end{cases} \quad (4.4)$$

where  $\mathbf{u} = [u_1, u_2]^T$  and  $\mathbf{B} = [B_1, B_2]^T$ . The above equation system is supplemented with homogeneous boundary conditions.

$$\begin{cases} \mathbf{u} = 0, & \mathbf{x} \in \partial\Omega, \end{cases} \quad (4.5)$$

$$\begin{cases} \mathbf{B} \cdot \mathbf{n} = 0, & \operatorname{curl} \mathbf{B} = 0, & \mathbf{x} \in \partial\Omega, \end{cases} \quad (4.6)$$

and initial conditions

$$\mathbf{u}(\mathbf{x}, 0) = \mathbf{u}_0(\mathbf{x}), \quad \mathbf{B}(\mathbf{x}, 0) = \mathbf{B}_0(\mathbf{x}), \quad (4.7)$$

where  $\operatorname{div} \mathbf{u}_0(\mathbf{x}) = \operatorname{div} \mathbf{B}_0(\mathbf{x}) = 0$ . It should be remarked that the two-dimensional incompressible MHD equations can be reformulated into scalar form with vorticity and magnetic stream functions, i.e., the  $\omega - \psi$  formulation, see [10]. However, for consistency with the original three-dimensional model, we still use (4.1)-(4.7). Analogous to the three-dimensional scheme, the linearized backward Euler FEM for (4.1)-(4.7) is to look for  $(\mathbf{u}_h^n, \mathbf{B}_h^n, p_h^n) \in \mathbf{X}_h^k \times \mathbf{Q}_h^k \times M_h^k$  with  $(p_h^n, 1) = 0$ , such that for any  $(\mathbf{v}_h, \mathbf{C}_h, q_h) \in \mathbf{X}_h^k \times \mathbf{Q}_h^k \times M_h^k$

$$\begin{cases} (D_\tau \mathbf{u}_h^n, \mathbf{v}_h) + \frac{1}{R_e} (\nabla \bar{\mathbf{u}}_h^n, \nabla \mathbf{v}_h) + \frac{1}{2} [(\mathbf{u}_h^{n-1} \cdot \nabla \bar{\mathbf{u}}_h^n, \mathbf{v}_h) - (\mathbf{u}_h^{n-1} \cdot \nabla \mathbf{v}_h, \bar{\mathbf{u}}_h^n)] \\ \quad - (p_h^n, \nabla \cdot \mathbf{v}_h) + S_c (\operatorname{curl} \bar{\mathbf{B}}_h^n, (\mathbf{B}_h^{n-1})^T \mathbb{T}_{\pi/2} \mathbf{v}_h) = (\mathbf{f}^n, \mathbf{v}_h) \end{cases} \quad (4.8)$$

$$\begin{cases} (D_\tau \mathbf{B}_h^n, \mathbf{C}_h) + \frac{S_c}{R_m} (\operatorname{curl} \bar{\mathbf{B}}_h^n, \operatorname{curl} \mathbf{C}_h) - S_c ((\mathbf{B}_h^{n-1})^T \mathbb{T}_{\pi/2} \bar{\mathbf{u}}_h^n, \operatorname{curl} \mathbf{C}_h) = 0, \end{cases} \quad (4.9)$$

$$\begin{cases} (\nabla \cdot \bar{\mathbf{u}}_h^n, q_h) = 0, \end{cases} \quad (4.10)$$

where  $\mathbb{T}_{\pi/2}$  is the rotation matrix defined by

$$\mathbb{T}_{\pi/2} = \begin{bmatrix} 0 & -1 \\ 1 & 0 \end{bmatrix}.$$

Again, we take  $\mathbf{u}_h^0 = \Pi_h \mathbf{u}^0$  and  $\mathbf{B}_h^0 = \Pi_h \mathbf{B}^0$  at the initial time step.

**Example 4.1** We test the performance of the proposed scheme (4.8)-(4.10) for a two-dimensional Hartmann flow problem, see [22]. We set  $\Omega = (0, 1)^2$  and  $R_e = S_c = R_m = 1.0$  in this example. The Hartmann flow problem has an explicit analytic solution as follows

$$\mathbf{u} = (u_1, 0)^T, \quad p = -x - \frac{(B_1)^2}{2}, \quad \mathbf{B} = (B_1, 1)^T, \quad (4.11)$$

where

$$u_1 = \frac{\cosh(\frac{1}{2}) - \cosh(y)}{2 \sinh(\frac{1}{2})}, \quad B_1 = \frac{\sinh(y) - 2 \sinh(\frac{1}{2}) y}{2 \sinh(\frac{1}{2})}.$$

It should be noted that the expressions (4.11) satisfy the following stationary incompressible MHD equations

$$\begin{cases} -\Delta \mathbf{u} + \mathbf{u} \cdot \nabla \mathbf{u} + \nabla p - \operatorname{curl} \mathbf{B} \begin{bmatrix} -B_2 \\ B_1 \end{bmatrix} = \mathbf{0}, & \mathbf{x} \in \Omega, & (4.12) \\ \operatorname{curl}(\operatorname{curl} \mathbf{B}) - \operatorname{curl}(u_1 B_2 - u_2 B_1) = \mathbf{0}, & \mathbf{x} \in \Omega, & (4.13) \\ \nabla \cdot \mathbf{u} = 0, & \mathbf{x} \in \Omega, & (4.14) \\ \nabla \cdot \mathbf{B} = 0, & \mathbf{x} \in \Omega. & (4.15) \end{cases}$$

However, the exact solution (4.11) does not fulfill the boundary condition (4.5)-(4.6) and constraint  $(p, 1) = 0$ . Therefore, we simply take the Dirichlet boundary condition based on the analytic solutions for  $\mathbf{u}_h^n$  and  $\mathbf{B}_h^n$ , while we set  $p_h^n = p(0, 0)$  on the node at the Origin. For the initial solution, we take

$$\mathbf{u} = (1, 0)^T, \quad \mathbf{B} = (0, 1)^T. \quad (4.16)$$

In the computation, we set  $\tau = 0.005$  and use  $\mathbf{X}_h^2 \times \mathbf{Q}_h^2 \times M_h^1$  on a uniform triangular mesh generated by FEniCS with  $h = \frac{1}{128}$ .

The numerical results obtained at  $T = 10$  are shown in Figure 1. It is easy to see that the numerical results computed by the proposed linearized mixed FEM agree well with [22], where a divergence free scheme was used to solve the incompressible MHD equations. We also plot The error functions in Figure 2.

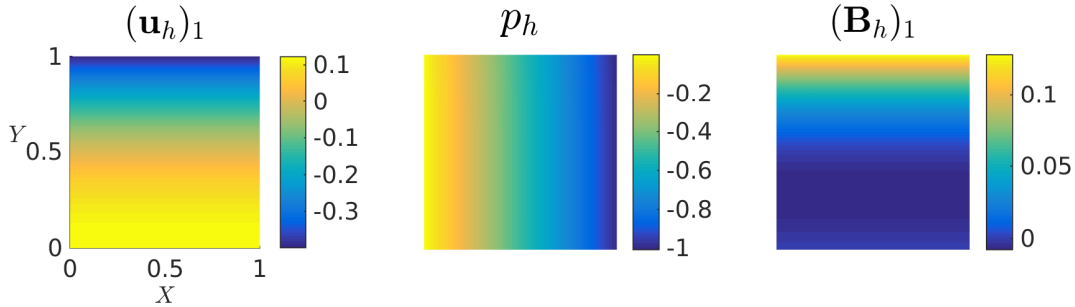


Figure 1: Numerical results of  $(\mathbf{u}_h)_1$ ,  $p_h$  and  $(\mathbf{B}_h)_1$  at  $T = 10$  computed by (4.8)-(4.10) with  $\tau = 0.005$  and  $h = 1/128$ . (Example 4.1)

## 4.2 Three-dimensional numerical experiments

**Example 4.2** In this example, we test the convergence of the proposed scheme (2.4)-(2.6) for a three-dimensional artificial problem. Here  $\Omega = (0, 1)^3$  and  $R_e = S_c = R_m = 1.0$ . The exact solution is taken to be

$$\mathbf{u} = \begin{bmatrix} e^t \cos(y) \\ e^t \cos(z) \\ e^t \cos(x) \end{bmatrix}, \quad p = e^t(x - 0.5) \cos(y) \sin(z), \quad \mathbf{B} = \begin{bmatrix} e^t \sin(y) \\ e^t \sin(z) \\ e^t \cos(x) \end{bmatrix}. \quad (4.17)$$

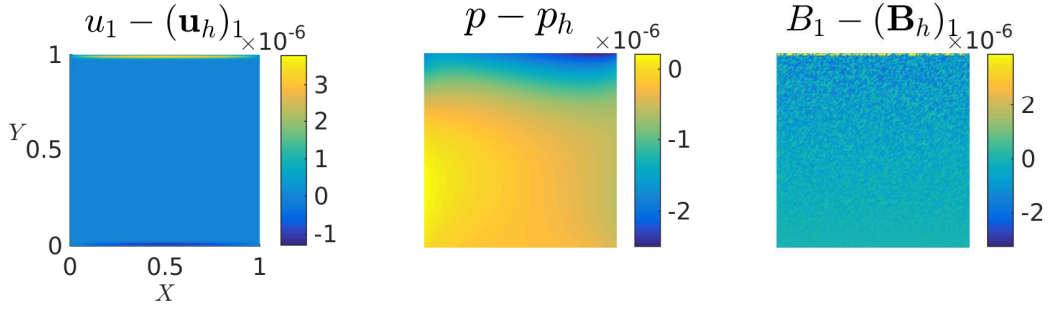


Figure 2: Error plots of  $(\mathbf{u}_h)_1$ ,  $p_h$  and  $(\mathbf{B}_h)_1$  at  $T = 10$  by (4.8)-(4.10) with  $\tau = 0.005$  and  $h = 1/128$ . (Example 4.1)

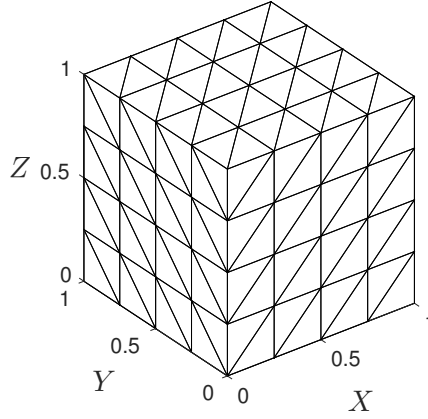


Figure 3: An illustration of uniform tetrahedral mesh with  $M = 4$ . (Example 4.2)

Here, one can verify that  $(p, 1) = 0$ . A uniform mesh is used in our computation. In each direction, there are  $M + 1$  vertices and therefore  $h = \sqrt{3}/M$ , see Figure 3 for illustration when  $M = 4$ .

To show the optimal convergence rate of the proposed method, we take  $\tau = \frac{1}{2M}$  for the lowest order method  $\mathbf{X}_h^2 \times \mathbf{Q}_h^1 \times M_h^1$  and  $\tau = \frac{1}{M^2}$  for  $\mathbf{X}_h^2 \times \mathbf{Q}_h^2 \times M_h^1$ , respectively. The  $L^2$  errors are shown in Table 1, where first order convergence for  $\mathbf{X}_h^2 \times \mathbf{Q}_h^1 \times M_h^1$  and second order convergence for  $\mathbf{X}_h^2 \times \mathbf{Q}_h^2 \times M_h^1$  are obtained. Numerical results from Table 1 verified that the proposed linearized scheme has optimal convergence rate, provided that the exact solution is smooth enough.

**Example 4.3** In the final example, we test the performance of the proposed scheme for a benchmark lid driven cavity problem on the unit cube domain  $\Omega = (0, 1)^3$  see Figure 4. Here, the physical parameters are chosen to satisfy the following incompressible MHD

Table 1:  $L^2$ -norm errors for the linearized scheme on the unit cube. (Example 4.2)

$\mathbf{X}_h^2 \times \mathbf{Q}_h^1 \times M_h^1 \quad (\tau = \frac{1}{2M})$						
	$\ \mathbf{u}_h^N - \mathbf{u}\ _{L^2}$	Order	$\ p_h^N - p\ _{L^2}$	Order	$\ \mathbf{B}_h^N - \mathbf{B}\ _{L^2}$	Order
M= 4	6.4876e-03	—	4.4078e-01	—	2.6777e-01	—
M= 8	3.3178e-03	0.9674	2.2073e-01	0.9978	1.3366e-01	1.0024
M= 16	1.6613e-03	0.9979	1.1004e-01	1.0043	6.6819e-02	1.0002
$\mathbf{X}_h^2 \times \mathbf{Q}_h^2 \times M_h^1 \quad (\tau = \frac{1}{M^2})$						
	$\ \mathbf{u}_h^N - \mathbf{u}\ _{L^2}$	Order	$\ p_h^N - p\ _{L^2}$	Order	$\ \mathbf{B}_h^N - \mathbf{B}\ _{L^2}$	Order
M= 4	3.2879e-03	—	2.0861e-01	—	4.2069e-02	—
M= 8	8.3121e-04	1.9839	5.3957e-02	1.9509	1.0361e-02	2.0216
M= 16	2.0776e-04	2.0003	1.3611e-02	1.9870	2.5797e-03	2.0059

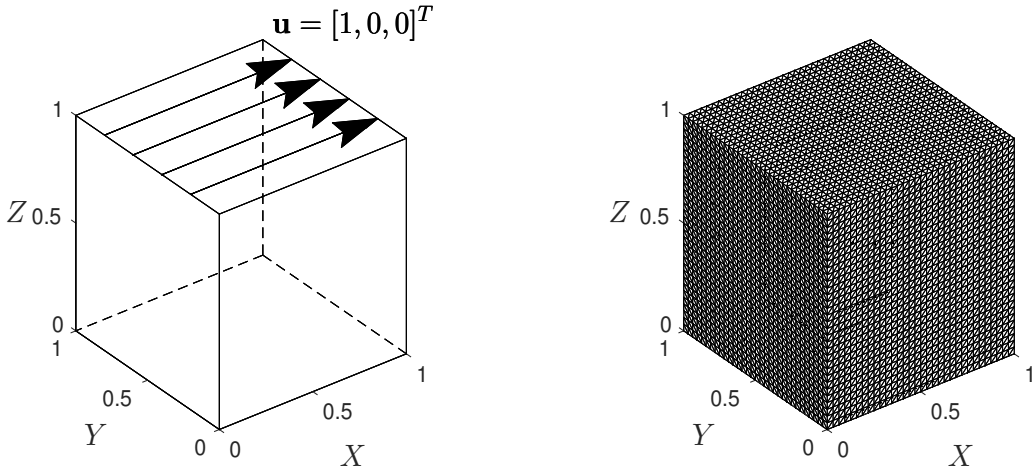


Figure 4: Left: illustration of the problem. Right: the mesh used in the computation,  $M = \frac{1}{32} 35,937$  nodes, 196,608 elements. 238,688 edges and 399,360 faces. (Example 4.3)

equations

$$\begin{cases} \frac{\partial \mathbf{u}}{\partial t} - \frac{1}{100} \Delta \mathbf{u} + \mathbf{u} \cdot \nabla \mathbf{u} + \nabla p - \frac{1}{20} \mathbf{curl} \mathbf{B} \times \mathbf{B} = \mathbf{f}, & \mathbf{x} \in \Omega, & (4.18) \\ \frac{\partial \mathbf{B}}{\partial t} + \frac{1}{200} \mathbf{curl}(\mathbf{curl} \mathbf{B}) - \mathbf{curl}(\mathbf{u} \times \mathbf{B}) = \mathbf{0}, & \mathbf{x} \in \Omega, & (4.19) \\ \nabla \cdot \mathbf{u} = 0, & \mathbf{x} \in \Omega, & (4.20) \\ \nabla \cdot \mathbf{B} = 0, & \mathbf{x} \in \Omega, & (4.21) \end{cases}$$

The initial conditions are taken to be

$$\mathbf{u}_0 = (v, 0, 0)^T, \quad \mathbf{B}_0 = (1, 0, 0)^T \quad (4.22)$$

where

$$v(x, y, z) = \begin{cases} (1 + \frac{1}{\alpha}(z-1))^2, & z \geq 1 - \alpha, \quad \alpha = 0.001, \\ 0, & \text{otherwise} \end{cases} \quad (4.23)$$

The boundary condition on  $\partial\Omega$  are set to be

$$\mathbf{u} = \mathbf{u}_0, \quad \mathbf{B} \cdot \mathbf{n} = 0, \quad \text{curl } \mathbf{B} \times \mathbf{n} = \mathbf{0}. \quad (4.24)$$

This example was tested in [21], where a divergence free approach was used. Some similar and simplified two-dimensional model were tested by several authors with different methods, e.g., see [25, 29, 34]. It should be noted that due to the different nondimensionalization procedure, the unknown  $\mathbf{B}$  in the above MHD equations (4.18)-(4.21) is a little bit different with the one used in (1.1)-(1.4). However, the scheme can be applied to (4.18)-(4.21) with a slight modification on the coefficients.

In the computation, we use  $\mathbf{X}_h^2 \times \mathbf{Q}_h^2 \times M_h^1$  on a uniform tetrahedral mesh with  $M = 32$ . There are 823,875 dofs for  $\mathbf{u}_h$ , 35,937 dofs for  $p_h$  and 1,276,096 dofs for  $\mathbf{B}_h$ , respectively. The time step  $\tau = 0.01$  is used in the computation.

As numerical results reported in [21, Example 5.4], shows that the stationary state arrives at  $T = 4$ , we show the numerical results at  $T = 4$  in Figures 5 and streamline of  $\mathbf{u}_h$  and at  $y = 0.5$  in Figure 5. Numerical experiments with finer time step  $\tau = 0.005$  have been done to verify the streamline pattern. From Figures 5, we see that the streamline at  $y = 0.5$  obtained by the proposed scheme (2.4)-(2.6) is very similar to those reported in [21, Example 5.4], where a divergence free scheme was used. The pressure contour plots in Figure 6 also agree well with previous results in [21, Example 5.4].

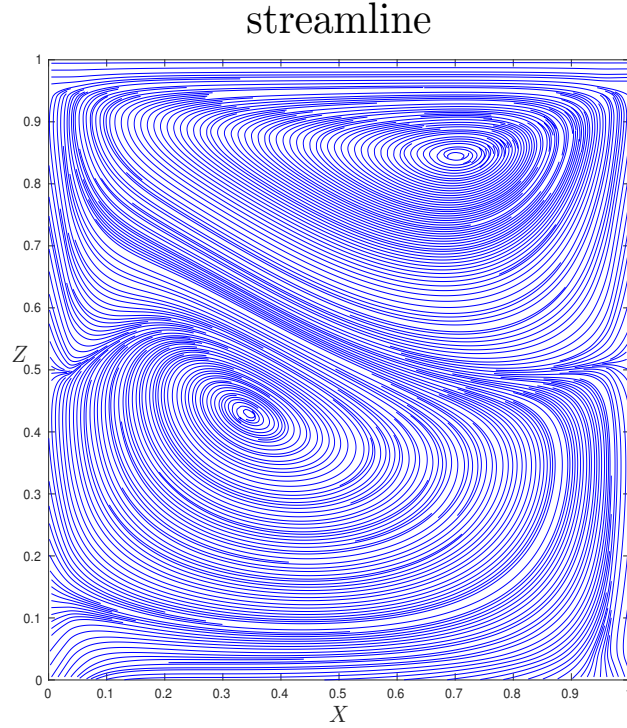


Figure 5: Streamline of  $\mathbf{u}_h$  at  $y = 0.5$ ,  $T = 4.0$ . Computed by  $\mathbf{X}_h^2 \times \mathbf{Q}_h^2 \times M_h^1$  on a uniform mesh with  $M = \frac{1}{32}$ ,  $\tau = 0.01$ . (Example 4.3)

As time evolves, we observe that the numerical solutions reach the stationary state

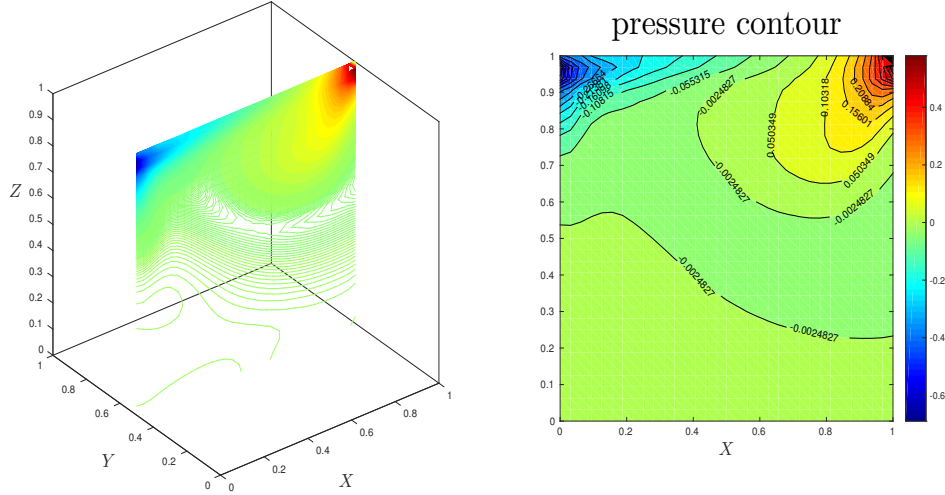


Figure 6: Pressure contour of  $p_h$  at  $y = 0.5$ ,  $T = 4.0$ . Computed by  $\mathbf{X}_h^2 \times \mathbf{Q}_h^2 \times M_h^1$  on a uniform mesh with  $M = \frac{1}{32}$ ,  $\tau = 0.01$ . (Example 4.3)

around  $T = 10.0$  with relative error

$$\frac{\|\mathbf{u}_h^n - \mathbf{u}_h^{n-1}\|_{L^2}}{\|\mathbf{u}_h^n\|_{L^2}} + \frac{\|p_h^n - p_h^{n-1}\|_{L^2}}{\|p_h^n\|_{L^2}} + \frac{\|\mathbf{B}_h^n - \mathbf{B}_h^{n-1}\|_{L^2}}{\|\mathbf{B}_h^n\|_{L^2}} = 1.067 \times 10^{-4}. \quad (4.25)$$

We present the streamline and pressure plots at  $T = 10.0$  in Figures 7 and 8, which are different with the results [21, Example 5.4]. In our computation, the error (4.25) at  $T = 10.0$  still decreases as time evolves, however, with an extremely slow decay rate (around  $10^{-7}$  for each time step).

## 5 Conclusions and remarks

The point of view that has been favored in some previous works is that violating the divergence constraint at the discrete level might lead to loss of energy preserving, which then result in nonphysical numerical solutions. However, we show in this paper that the energy preserving still holds without satisfying the point-wise divergence free condition. Furthermore, numerical experiments for the Hartmann flow and the lid-driven cavity incompressible MHD flow demonstrate that the proposed scheme provide numerical results as good as that obtained by schemes satisfying  $\text{div} \mathbf{B}_h = 0$ .

In this paper, we use a linearized backward Euler scheme, which is first order accurate in the temporal direction. The main reason is that, for the incompressible MHD problem, the large storage is a crucial issue in the three-dimensional space. There are many ways to design higher order integrator. For instance, a second order linearized FEM is to look for

## streamline

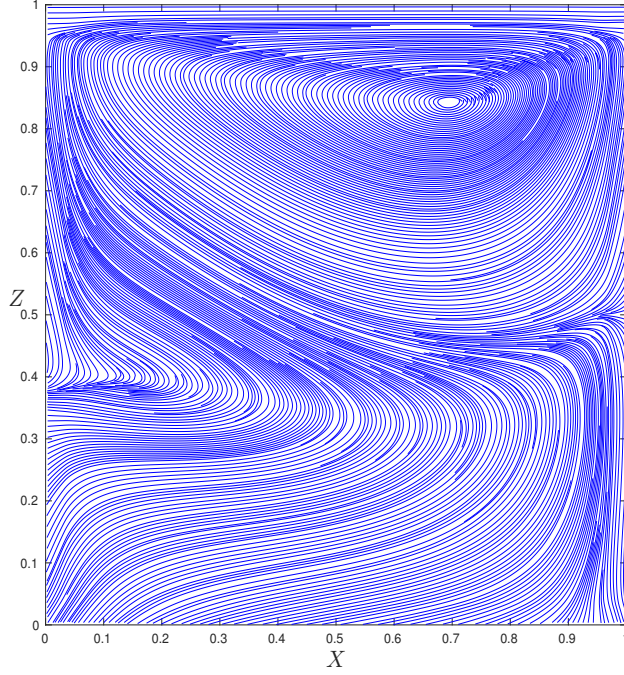


Figure 7: Streamline of  $\mathbf{u}_h$  at  $y = 0.5$ ,  $T = 10.0$ . Computed by  $\mathbf{X}_h^2 \times \mathbf{Q}_h^2 \times M_h^1$  on a uniform mesh with  $M = \frac{1}{32}$ ,  $\tau = 0.01$ . (Example 4.3)

$(\mathbf{u}_h^n, \mathbf{B}_h^n, p_h^n) \in \mathbf{X}_h^k \times \widehat{\mathbf{Q}}_h^k \times M_h^k$ , such that for any  $(\mathbf{v}_h, \mathbf{C}_h, q_h) \in \mathbf{X}_h^k \times \widehat{\mathbf{Q}}_h^k \times M_h^k$

$$\begin{cases} \frac{1}{\tau} \left( \frac{3}{2} \mathbf{u}_h^n - 2\mathbf{u}_h^{n-1} - \frac{1}{2} \mathbf{u}_h^{n-2}, \mathbf{v}_h \right) + \frac{1}{Re} (\nabla \mathbf{u}_h^n, \nabla \mathbf{v}_h) + \frac{1}{2} [(\widehat{\mathbf{u}}_h^n \cdot \nabla \mathbf{u}_h^n, \mathbf{v}_h) - (\widehat{\mathbf{u}}_h^n \cdot \nabla \mathbf{v}_h, \mathbf{u}_h^n)] \\ \quad - (p_h^n, \nabla \cdot \mathbf{v}_h) - S_c (\mathbf{curl} \mathbf{B}_h^n \times \widehat{\mathbf{B}}_h^n, \mathbf{v}_h) = (\mathbf{f}^n, \mathbf{v}_h), \\ \frac{1}{\tau} \left( \frac{3}{2} \mathbf{B}_h^n - 2\mathbf{B}_h^{n-1} + \frac{1}{2} \mathbf{B}_h^{n-2}, \mathbf{C}_h \right) + \frac{S_c}{R_m} (\mathbf{curl} \mathbf{B}_h^n, \mathbf{curl} \mathbf{C}_h) - S_c (\mathbf{u}_h^n \times \widehat{\mathbf{B}}_h^n, \mathbf{curl} \mathbf{C}_h) = 0, \\ (\nabla \cdot \mathbf{u}_h^n, q_h) = 0, \end{cases}$$

where  $\widehat{\mathbf{u}}_h^n = 2\mathbf{u}_h^{n-1} - \mathbf{u}_h^{n-2}$  and  $\widehat{\mathbf{B}}_h^n = 2\mathbf{B}_h^{n-1} - \mathbf{B}_h^{n-2}$ . For this three-level method, the linearized backward Euler FEM (2.4)-(2.6) can be used to compute  $(\mathbf{u}_h^1, \mathbf{B}_h^1, p_h^1)$ . We shall also remark that, an  $L^2$  error estimates of  $O(\tau^2 + h^s)$  can be obtained by a similar analysis, provided enough temporal regularity. We focus on the homogeneous boundary condition (1.5)-(1.6) in this paper. It should be noted that the boundary condition (1.8) can be easily implemented with the Nédélec edge element. All the theoretical results can be extended to models with more complicated boundary conditions.

## Acknowledgment

The authors would like to thank Mr. Ben Dai and Prof. Junhui Wang for help on conducting the numerical experiments.

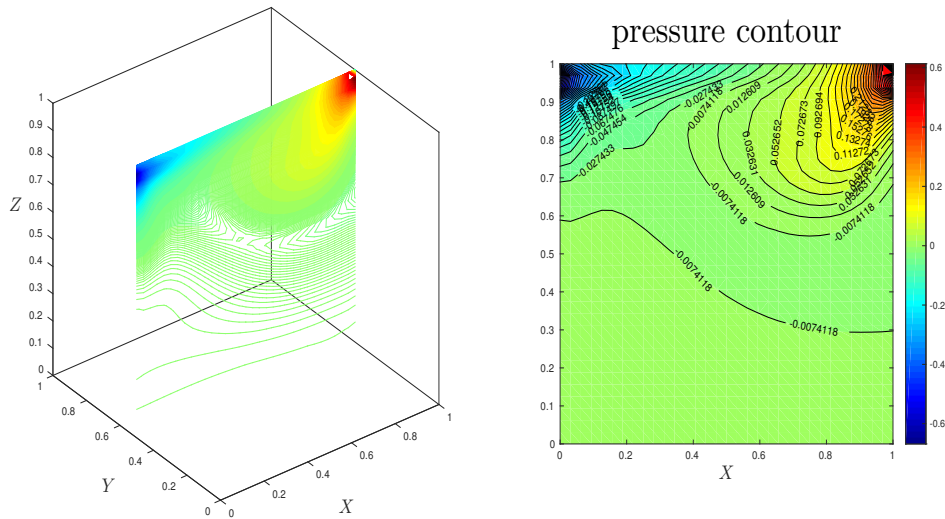


Figure 8: Pressure contour of  $p_h$  at  $y = 0.5$ ,  $T = 10.0$ . Computed by  $\mathbf{X}_h^2 \times \mathbf{Q}_h^2 \times M_h^1$  on a uniform mesh with  $M = \frac{1}{32}$ ,  $\tau = 0.01$ . (Example 4.3)

## References

- [1] C. Amrouche, C. Bernardi, M. Dauge and V. Girault, Vector potentials in three-dimensional nonsmooth domains, *Math. Meth. Appl. Sci.*, 21(1998), pp. 823–864.
- [2] A. Alonso and A. Valli, An optimal domain decomposition preconditioner for low-frequency time-harmonic Maxwell equations. *Math. Comp.*, 68(1999), pp 607–631.
- [3] S. Badia, R. Codina and R. Planas On an unconditionally convergent stabilized finite element approximation of resistive magnetohydrodynamics, *J. Comput. Phys.*, 234(2013), pp. 399–416.
- [4] J. Bergh and J. Lofstrom, *Interpolation spaces: An introduction*, Springer–Verlag, Berlin–New York, 1976.
- [5] D. Boffi, F. Brezzi and M. Fortin, *Mixed Finite Element Methods and Applications*, Springer, Heidelberg, 2013.
- [6] J. Brackbill and D. Barnes, The effect of nonzero  $\text{div}\mathbf{B}$  on the numerical solution of the Magnetohydrodynamic equations, *J. Comput. Phys.*, 35(1980), pp. 426–430.
- [7] S. Brenner and L. Scott, *The Mathematical Theory of Finite Element Methods*, Springer, New York, 2002.
- [8] P. Chatzipantelidis, R.D. Lazarov, V. Thomée and L.B. Wahlbin, Parabolic finite element equations in nonconvex polygonal domains, *BIT Numer. Math.*, 46(2006), pp. S113–S143.

- [9] K. Chrysafinos and L. Hou, Error estimates for semidiscrete finite element approximations of linear and semilinear parabolic equations under minimal regularity assumptions, *SIAM J. Numer. Anal.*, 40(2002), pp. 282–306.
- [10] D. Cordoba and C. Marliani, On the behavior of hyperbolic neutral points in two-dimensional ideal magnetohydrodynamics, *Proc. Natl. Acad. Sci. USA*, 96(1999), pp. 2612–2614.
- [11] R. Codina and N. Hernández-Silva, Stabilized finite element approximation of the stationary magneto-hydrodynamics equations, *Comput. Mech.*, 38(2006), pp. 344–355.
- [12] M. Costabel and M. Dauge, Singularities of electromagnetic fields in polyhedral domains. *Arch. Rational Mech. Anal.*, 151(2000), pp. 221–276.
- [13] J. Gerbeau, C. Le Bris and T. Lelièvre, *Mathematical Methods for the Magnetohydrodynamics of Liquid Metals*, Oxford University Press, Oxford, 2006.
- [14] C. Greif, D. Li, D. Schötzau, X. Wei, A mixed finite element method with exactly divergence-free velocities for incompressible magnetohydrodynamics, *Comput. Methods Appl. Mech. Engrg.*, 199(2010), pp. 2840–2855.
- [15] V. Girault and P. Raviart, *Finite Element Method for Navier–Stokes Equations: Theory and Algorithms*, Springer–Verlag, Berlin, Heidelberg, 1987.
- [16] J. Goedbloed and S. Poedts, *Principles of Magnetohydrodynamics with Applications to Laboratory and Astrophysical Plasmas*, Cambridge University Press, Cambridge, MA, 2004.
- [17] M. Gunzburger, A. Meir and J. Peterson, On the existence, uniqueness, and finite element approximation of solutions of the equations of stationary, incompressible magnetohydrodynamics, *Math. Comp.*, 56(1991), pp. 523–563.
- [18] U. Hasler, A. Schneebeli and D. Schötzau, Mixed finite element approximation of incompressible MHD problems based on weighted regularization, *Appl. Numer. Math.*, 51(2004), pp. 19–45.
- [19] J. Heywood and R. Rannacher, Finite element approximation of the nonstationary Navier–Stokes problem IV: Error analysis for second-order time discretization, *SIAM J. Numer. Anal.*, 27(1990), pp. 353–384.
- [20] Y. He, Unconditional convergence of the Euler semi-implicit scheme for the three-dimensional incompressible MHD equations, *IMA J. Numer. Anal.*, 35(2015), pp. 767–801.
- [21] R. Hiptmair, M. Li, S. Mao and W. Zheng, A fully divergence-free finite element method for magnetohydrodynamic equations, preprint, <https://www.math.ethz.ch/sam/research/reports.html?year=2017>
- [22] K. Hu, Y. Ma and J. Xu, Stable finite element methods preserving  $\nabla \cdot \mathbf{B} = 0$  exactly for MHD models, *Numer. Math.*, 135(2017), pp. 371–396.
- [23] F. Lin and P. Zhang, Global small solutions to an MHD-type system: the three-dimensional case. *Comm. Pure Appl. Math.*, 67(2014), pp. 531–580.

- [24] A. Logg, K. Mardal, and G. Wells (Eds.), *Automated Solution of Differential Equations by the Finite Element Method*, Springer, Berlin, 2012.
- [25] L. Marioni, F. Bay and E. Hachem, Numerical stability analysis and flow simulation of lid-driven cavity subjected to high magnetic field, *Phys. Fluids*, 28(2016), pp. 057102.
- [26] P. Monk, *Finite Element Methods for Maxwell's Equations*, Oxford University Press, New York, 2003.
- [27] R. Moreau, *Magnetohydrodynamics*, Kluwer Academic Publishers, New York, 1990.
- [28] L. Nirenberg, An extended interpolation inequality, *Ann. Scuola Norm. Sup. Pisa (3)*, 20(1966), pp. 733–737.
- [29] E. Phillips, H. Elman, E. Cyr, J. Shadid and R. Pawlowski, Block preconditioners for stable mixed nodal and edge finite element representations of incompressible resistive MHD, *SIAM J. Sci. Comput.*, 36(2016), pp. B1009–B1031.
- [30] A. Prohl, Convergent finite element discretizations of the nonstationary incompressible magnetohydrodynamics system, *M2AN Math. Model. Numer. Anal.*, 42(2008), pp. 1065–1087.
- [31] D. Schötzau, Mixed finite element methods for stationary incompressible magnetohydrodynamics, *Numer. Math.*, 96(2004), pp. 771–800.
- [32] M. Schonbek, T. Schonbek, and E. Söli, Large-time behaviour of solutions to the magnetohydrodynamics equations, *Math. Ann.*, 304(1996), pp. 717–756.
- [33] M. Sermene and R. Temam, Some mathematics questions related to the MHD equations, *Commun. Pure Appl. Math.*, XXXIV(1984), pp. 635–664.
- [34] V. Shatrov, G. Mutschke and G. Gerberth, Three-dimensional linear stability analysis of lid-driven magnetohydrodynamic cavity flow, *Phys. Fluids*, 15(2003), pp. 2141–2151.
- [35] G. Zhang, J. Yang and C. Bi, Second order unconditionally convergent and energy stable linearized scheme for MHD equations, *Adv. Comput. Math.*, DOI: 10.1007/s10444-017-9552-x.